



Search for third-generation scalar leptoquarks in the $t\tau$ channel in proton-proton collisions at $\sqrt{s} = 8$ TeV

The CMS Collaboration*

Abstract

A search for pair production of third-generation scalar leptoquarks decaying to top quark and τ lepton pairs is presented using proton-proton collision data at a center-of-mass energy of $\sqrt{s} = 8$ TeV collected with the CMS detector at the LHC and corresponding to an integrated luminosity of 19.7 fb^{-1} . The search is performed using events that contain an electron or a muon, a hadronically decaying τ lepton, and two or more jets. The observations are found to be consistent with the standard model predictions. Assuming that all leptoquarks decay to a top quark and a τ lepton, the existence of pair produced, charge $-1/3$, third-generation leptoquarks up to a mass of 685 GeV is excluded at 95% confidence level. This result constitutes the first direct limit for leptoquarks decaying into a top quark and a τ lepton, and may also be applied directly to the pair production of bottom squarks decaying predominantly via the R-parity violating coupling λ'_{333} .

Published in the Journal of High Energy Physics as doi:10.1007/JHEP07(2015)042.

arXiv:1503.09049v3 [hep-ex] 21 Nov 2016

1 Introduction

Leptoquarks (LQ) are hypothetical particles that carry both lepton (L) and baryon (B) quantum numbers. They appear in theories beyond the standard model (SM), such as grand unification [1–3], technicolor [4], and compositeness [5, 6] models. A minimal extension of the SM to include all renormalizable gauge invariant interactions, while respecting existing bounds from low-energy and precision measurements leads to the effective Buchmüller–Rückl–Wyler model [7]. In this model, LQs are assumed to couple to one generation of chiral fermions, and to separately conserve L and B quantum numbers. An LQ can be either a scalar (spin 0) or a vector (spin 1) particle with a fractional electric charge. A comprehensive list of other possible quantum number assignments for LQs coupling to SM fermions can be found in Ref. [8].

This paper presents the first search for a third-generation scalar LQ (LQ_3) decaying into a top quark and a τ lepton. Previous searches at hadron colliders have targeted LQs decaying into quarks and leptons of the first and second generations [9–11] or the third-generation in the $LQ_3 \rightarrow b\nu$ and $LQ_3 \rightarrow b\tau$ decay channels [12–17]. The presented search for third-generation LQs can also be interpreted in the context of R-parity violating (RPV) supersymmetric models [18] where the supersymmetric partner of the bottom quark (bottom squark) decays into a top quark and a τ lepton via the RPV coupling λ'_{333} .

At hadron colliders, such as the CERN LHC, LQs are mainly pair produced through the quantum chromodynamic (QCD) quark-antiquark annihilation and gluon-gluon fusion subprocesses. There is also a lepton mediated $t(u)$ -channel contribution that depends on the unknown lepton-quark-LQ Yukawa coupling, but this contribution is suppressed at the LHC for the production of third-generation LQs as it requires third-generation quarks in the initial state. Hence, the LQ pair production cross section depends only upon the assumed values of the LQ spin and mass, and upon the proton-proton center-of-mass energy. We consider scalar LQs in the mass range up to several hundred GeV. The corresponding next-to-leading-order (NLO) pair production cross sections and associated uncertainties at $\sqrt{s} = 8$ TeV are taken from the calculation presented in Ref. [19].

It is customary to denote the branching fractions of LQs into a quark and a charged lepton or a quark and a neutrino within the same generation as β and $1 - \beta$, respectively. Assuming that third-generation scalar LQs with charge $-1/3$ exclusively couple to quarks and leptons of the third-generation, the two possible decay channels are $LQ_3 \rightarrow t\tau^-$ and $LQ_3 \rightarrow b\nu$. In this paper, we initially assume that $\beta = 1$ so that the LQ_3 always decays to a $t\tau$ pair. The results are then reinterpreted as a function of the branching fraction with β treated as a free parameter.

We consider events with at least one electron or muon and one τ lepton where the τ lepton undergoes a one- or three-prong hadronic decay, $\tau_h \rightarrow \text{hadron}(s) + \nu_\tau$. In $LQ_3\bar{L}Q_3$ decays, τ leptons arise directly from LQ decays, as well as from W bosons in the top quark decay chain, whereas electrons and muons are produced only in leptonic decays of W bosons or τ leptons. The major backgrounds come from $t\bar{t}$ +jets, Drell–Yan(DY)+jets, and W+jets production, where a significant number of events have jets misidentified as hadronically decaying τ leptons. The search is conducted in two orthogonal selections, labelled as category A and category B. In category A, a same-sign $\mu\tau_h$ pair is required in each event, which suppresses SM backgrounds. Misidentified τ_h candidates originating from jets constitute the main background in category A. Category B utilizes both $e\tau_h$ and $\mu\tau_h$ pairs with slightly relaxed τ lepton identification criteria without imposing a charge requirement on the lepton pair. This yields a higher signal acceptance, but a larger irreducible background from SM processes. In order to keep the two samples statistically independent, events that satisfy the category A criteria are removed from the category B sample. Figure 1 shows a schematic representation of an $LQ_3\bar{L}Q_3$ decay chain

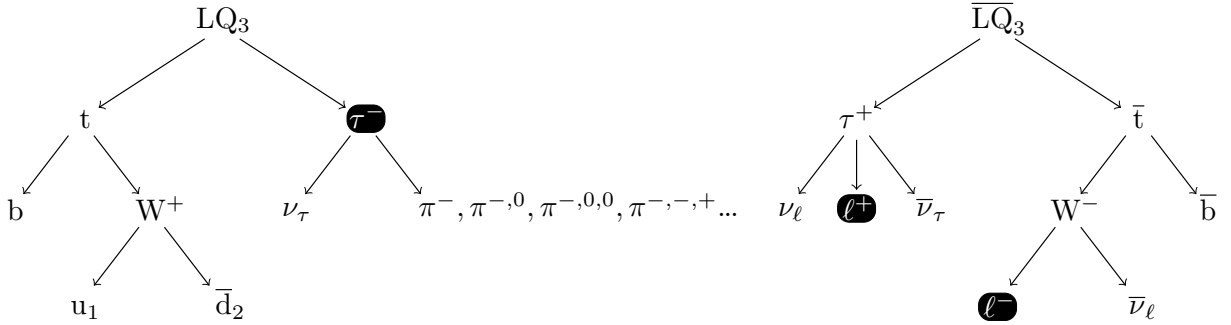


Figure 1: One of the $LQ_3\bar{LQ}_3$ decay chains with both same-sign and opposite-sign $\ell\tau_h$ pairs. Labels u and d denote up and down type quarks, and ℓ denotes an electron or a muon.

that can satisfy the requirements for both categories.

The signature for this search is chosen to be $\ell\tau_h+X$, where ℓ denotes an electron or a muon, and X is two or more jets and any additional charged leptons in category A, or three or more jets and any additional charged leptons in category B. The additional jet requirement in category B is beneficial in suppressing background events from dominant SM processes with two jets and an opposite-sign $\ell\tau_h$ pair.

2 Reconstruction and identification of physics objects

The CMS apparatus is a multipurpose particle detector with a superconducting solenoid of 6 m internal diameter, which provides a magnetic field of 3.8 T. Within the volume of the solenoid are a silicon pixel and strip tracker, a lead tungstate crystal electromagnetic calorimeter, and a brass and scintillator hadron calorimeter, each composed of a barrel and two endcap sections. Muons are measured in gas-ionization detectors embedded in the steel flux-return yoke outside the solenoid. Extensive forward calorimetry complements the coverage provided by the barrel and endcap detectors. A more detailed description of the CMS detector, together with a definition of the coordinate system used and the relevant kinematic variables, can be found in Ref. [20].

The electron, muon, and τ lepton candidates used in this paper are reconstructed using a particle-flow (PF) event reconstruction technique [21, 22] which reconstructs and identifies single particles (muons, electrons, charged/neutral hadrons, and photons) using an optimized combination of all subdetector information.

Muon candidates are reconstructed from a combined track in the muon system and the tracking system [23]. The hadronically decaying τ lepton candidates are reconstructed via the “hadron-plus-strips” algorithm which combines one or three charged hadrons with up to two neutral pions that are reconstructed from PF candidates combining tracker and calorimeter information [24]. Electron candidates are obtained by reconstructing trajectories from hits in the tracker layers and energy depositions in the electromagnetic calorimeter with a Gaussian sum filter [25].

Jets are reconstructed by using the anti- k_T algorithm [22, 26, 27] to cluster PF candidates with a distance parameter of $\Delta R = 0.5$ (where $\Delta R = \sqrt{(\Delta\eta)^2 + (\Delta\phi)^2}$, η denotes the pseudorapidity and ϕ denotes the azimuthal angle in radians). The missing transverse momentum \vec{p}_T^{miss} is calculated as a negative vectorial sum of the transverse momenta of all the PF candidates. The missing transverse energy E_T^{miss} is defined as the magnitude of the \vec{p}_T^{miss} vector. Jet energy corrections are applied to all jets and are also propagated to the calculation of E_T^{miss} [28].

The collisions are selected using a two-tiered trigger system, composed of a hardware based level-1 trigger and a software based high-level trigger (HLT) [29] running on a computing farm.

The following quantities are constructed using the physics objects described earlier:

- S_T is the scalar p_T sum of all objects in the event, including muons, hadronically decaying τ leptons, electrons, jets, and E_T^{miss} .
- $M_T(\ell, \vec{p}_T^{\text{miss}})$ is the transverse mass, $\sqrt{2p_T^\ell E_T^{\text{miss}}(1 - \cos(\Delta\phi(\vec{p}_T^{\text{miss}}, \ell)))}$, reconstructed from the given lepton and the \vec{p}_T^{miss} in the event where $\Delta\phi(\vec{p}_T^{\text{miss}}, \ell)$ is the difference in the azimuthal angle between the directions of the missing transverse momentum and the lepton momentum.
- $|\widetilde{\eta}|$ is the pseudorapidity defined as $|\widetilde{\eta}| = -\ln \tan(\bar{\theta}/2)$, where $\bar{\theta}$ is the average absolute polar angle of all electrons, muons, and hadronically decaying τ leptons in an event as measured from the beam-axis in the lab frame, and is used as a measure of the event centrality.

3 Data and simulated samples

This analysis uses data collected with the CMS detector at the LHC during proton-proton (pp) collisions at $\sqrt{s} = 8$ TeV. Proton bunches were separated by 50 ns and the average number of additional primary vertices in the collision of the two beams in the same proton bunch crossing was 20 (pileup). The search is conducted using a combination of isolated and non-isolated single-muon data corresponding to an integrated luminosity of 19.5 fb^{-1} in category A, and using isolated single-muon or single-electron data corresponding to an integrated luminosity of 19.7 fb^{-1} in category B. The muon triggers require a muon candidate to have $p_T > 24$ GeV and $|\eta| < 2.1$. The electron trigger requires an isolated electron candidate with $p_T > 27$ GeV and $|\eta| < 2.5$.

The LQ signal processes have been simulated using the PYTHIA generator (v6.426) [30]. Single top quark and top quark pair production have been simulated with POWHEG (v1.0) [31–34]. For the W +jets background, DY +jets processes, and $t\bar{t}$ production in association with W or Z bosons, MADGRAPH (v5.1) has been used [35]. Diboson and QCD multijet processes as well as processes involving Higgs bosons have been generated with PYTHIA, other SM backgrounds have been simulated with MADGRAPH. The parton shower and hadronization in samples generated with POWHEG or MADGRAPH has been performed with PYTHIA. In case of MADGRAPH, the matching to PYTHIA has been done with the MLM scheme [36]. In all of the generated samples, τ lepton decays were simulated via TAUOLA [37] and the response of the CMS detector has been simulated with GEANT4 [38]. The POWHEG samples are produced with the CT10 [39] parton distribution function (PDF), all other samples have been generated using CTEQ6L1 [40] PDF set. The Monte Carlo (MC) simulated events are re-weighted to account for differences in trigger and lepton reconstruction efficiencies, pileup modeling, and jet/missing transverse energy response of the detector. The simulated events are normalized using next-to-next-to-leading-order (NNLO) (W +jets, DY +jets [41], $t\bar{t}$ +jets [42], WH , ZH [43]), approximate NNLO (t , tW [44]), NLO (diboson [45], $t\bar{t}Z$ [46], $t\bar{t}W$ [46, 47], $t\bar{t}H$ [48, 49], triboson [50]), or leading-order ($W^\pm W^\pm qq$, $t\bar{t}WW$, $W\gamma^*$, QCD multijet [30, 35]) cross sections at $\sqrt{s} = 8$ TeV.

The characteristics of the simulated $t\bar{t}$ +jets and W +jets events have been found to contain discrepancies when compared with measurements of the p_T spectrum of top quarks [51] and the leading jet [52], respectively. Re-weighting factors, parametrized as functions of the respective p_T distributions, are applied to the simulated events to correct for these discrepancies. The

Table 1: Summary of the search strategies in event categories A and B.

	Category A	Category B
Lepton selection	Same-sign $\mu\tau_h$ pair	$\mu\tau_h$ or $e\tau_h$ pair (category A events are removed)
Jet selection	At least two jets	At least three jets
E_T^{miss} requirement	No E_T^{miss} requirement	$E_T^{\text{miss}} > 50$ GeV
S_T and τ lepton p_T requirements	Optimized for each LQ mass hypothesis	$S_T > 1000$ GeV, $p_T^\tau > 20$ GeV
Background estimation	Main component containing misidentified muons & τ leptons estimated using data events	Estimated via simulation, corrections applied for τ lepton misidentification rate and top quark and W p_T distributions
Search regions	2 search regions binned in $ \widetilde{\eta} $	8 search regions in 4 τ lepton p_T regions for $\mu\tau_h$ and $e\tau_h$ channels

correction factors for $t\bar{t}$ +jets [51] range up to 30% whereas the correction factors for the W +jets samples vary between 8% and 12%.

4 Event selection

A summary of the search regions, selection criteria, and the methods used to determine background contributions for categories A and B is given in Table 1.

4.1 Event selection in category A

In category A, two selections, denoted as loose and tight, are defined for the muon and τ lepton candidates, which differ only in the thresholds of the isolation requirements. The tight selections are applied to define the signal region, and the loose selections are used in the estimation of backgrounds as defined in Section 5.1.

Muon candidates are required to have $p_T > 25$ GeV and $|\eta| < 2.1$. The loose muon selection has no isolation requirement, whereas the tight muon selection requires the scalar p_T sum of all PF candidates in a cone of radius $\Delta R = 0.4$ around the muon to be less than 12% of the muon p_T . The muon kinematic and isolation thresholds are chosen to match the trigger requirements used in selecting the events.

Hadronically decaying τ lepton candidates are required to satisfy $p_T > 20$ GeV and $|\eta| < 2.1$. For the loose τ lepton selection, the scalar p_T sum of charged hadron and photon PF candidates with $p_T > 0.5$ GeV in a cone of radius $\Delta R = 0.3$ around the τ lepton candidate is required to be less than 3 GeV. For the tight τ lepton selection, a more restrictive isolation requirement is applied with a cone of radius $\Delta R = 0.5$ and a threshold value of 0.8 GeV [24]. All τ_h candidates are required to satisfy a requirement that suppresses the misidentification of electrons and muons as hadronically decaying τ leptons [24].

Electron candidates are required to have $p_T > 15$ GeV and $|\eta| < 2.5$. The ratio of the scalar p_T sum of all PF candidates in a cone of radius $\Delta R = 0.3$ around the electron object, relative to the electron p_T , is required to be less than 15%.

All muon, electron, and τ_h candidates are required to be separated by $\Delta R > 0.3$ from each other. In addition, the separation between the muon and τ lepton candidates and the nearest jet to which they do not contribute is required to be $\Delta R(\mu, j)_{\text{min}} > 0.5$ and $\Delta R(\tau, j)_{\text{min}} > 0.7$

respectively. This requirement is imposed in order to reduce the impact of QCD jet activity on the respective isolation cones.

Jet candidates are required to have $p_T > 40 \text{ GeV}$, $|\eta| < 3$. Jets overlapping with the electron, muon, and τ_h candidates within a cone of $\Delta R = 0.5$ are not considered.

Each event is required to contain a same-sign $\mu\tau_h$ pair, chosen among the muon and τ_h lepton candidates satisfying the loose selection criteria. If the event contains more than one $\mu\tau_h$ pair, the same-sign pair with the largest scalar sum p_T is selected. The selected $\mu\tau_h$ pair is then required to satisfy the tight selection criteria. Events failing the tight selection criteria on one or both leptons are utilized in the estimation of backgrounds described in Section 5.1.

For the signal selection, same-sign $\mu\tau_h$ events are required to have $S_T > 400 \text{ GeV}$ and two or more jets. Events containing an opposite-sign dimuon pair with an invariant mass within 10% of the Z boson mass are vetoed. In order to exploit a feature of the signal model that produces the LQ_3 pair dominantly in the central region, the search is split into two channels with $|\widetilde{\eta}| < 0.9$ (central) and $|\widetilde{\eta}| \geq 0.9$ (forward). Furthermore, a 2D optimization is performed using the simulated samples for the determination of selection criteria in the (S_T, p_T^τ) plane for each LQ_3 mass hypothesis in the range of 200–800 GeV. The p_T^τ requirement is only applied to the τ lepton candidate that is a part of the selected same-sign $\mu\tau_h$ pair. The optimization is accomplished by maximizing the figure of merit given in Eq. (1) [53]:

$$\chi(p_T^\tau, S_T) = \frac{\varepsilon(p_T^\tau, S_T)}{1 + \sqrt{B(p_T^\tau, S_T)}} \quad (1)$$

where ε is the signal efficiency and B is the number of background events. The (S_T, p_T^τ) thresholds have been optimized in the central channel and applied identically in the forward channel. These optimized selections and the corresponding efficiencies as a function of the LQ_3 mass are presented later, in Section 6.

A signal-depleted selection of events with a same-sign $\mu\tau_h$ pair, created by vetoing events with more than one jet, is used to check the performance and normalization of the simulated background samples. In order to reduce the QCD multijet background contribution, an additional requirement of $M_T(\mu, E_T^{\text{miss}}) > 40 \text{ GeV}$ is imposed using the muon candidate in the selected same-sign $\mu\tau_h$ pair. Figure 2 illustrates the agreement between data and simulation in the $|\widetilde{\eta}|$ and S_T distributions, which is found to be within 20%.

4.2 Event selection in category B

In category B, muon candidates are required to have $p_T > 30 \text{ GeV}$ and $|\eta| < 2.1$. The muon isolation requirement follows the tight muon selection defined for category A.

Hadronically decaying τ leptons must satisfy $p_T > 20 \text{ GeV}$ and $|\eta| < 2.1$. For τ_h candidates a medium isolation requirement is used, where the scalar p_T sum of PF candidates must not exceed 1 GeV in a cone of radius $\Delta R = 0.5$. As in category A, τ_h candidates must satisfy the requirement discriminating against misreconstructed electrons and muons.

Electron candidates are required to have $p_T > 35 \text{ GeV}$ and $|\eta| < 2.1$. The electron isolation requirement follows the description in category A, but with a tighter threshold at 10% in order to match the trigger isolation requirements in the $e\tau_h$ channel.

Jets are required to have $p_T > 30 \text{ GeV}$, $|\eta| < 2.5$, and those overlapping with τ_h candidates within a cone of $\Delta R = 0.5$ are ignored. Furthermore, τ leptons that overlap with a muon, and electrons that overlap with a jet within a cone of $\Delta R = 0.5$ are not considered.

Each event is required to have at least one electron or muon and one τ_h candidate. Events containing muons are vetoed in the $e\tau_h$ channel. Events satisfying the category A selection criteria are also vetoed, thus in the case of the $\mu\tau_h$ selection, category B mostly consists of events with opposite-sign $\mu\tau_h$ pairs.

In addition, events are required to have $S_T > 1000 \text{ GeV}$, $E_T^{\text{miss}} > 50 \text{ GeV}$, and at least three jets, where the leading and subleading jets further satisfy $p_T > 100$ and 50 GeV , respectively. The analysis in category B is performed in four search regions defined as a function of the transverse momentum of the leading τ_h candidate: $20 < p_T^\tau < 60 \text{ GeV}$, $60 < p_T^\tau < 120 \text{ GeV}$, $120 < p_T^\tau < 200 \text{ GeV}$, and $p_T^\tau > 200 \text{ GeV}$. Since events with $e\tau_h$ and $\mu\tau_h$ pairs are separated, this selection leads to eight search regions. The two low- p_T^τ regions are mainly used to constrain the SM background processes, whereas the signal is expected to populate the two high- p_T^τ regions. The selections on S_T , the momenta of the three jets, and E_T^{miss} have been optimized with respect to the expected limits on the signal cross section obtained in the statistical evaluation of the search regions as described in Section 6.

A signal-depleted selection is used to check the performance of the simulated background samples in category B. In this selection, events with $\ell\tau_h$ pairs are required to have $E_T^{\text{miss}} < 50 \text{ GeV}$ and at least two jets with $p_T > 50 \text{ GeV}$, $|\eta| < 2.5$. Figure 3 shows that in general the agreement between data and simulation is within the statistical uncertainties in the leading p_T^τ distributions. In the $e\tau_h$ channel, a small excess in the p_T distribution is observed around 150 GeV . As the other kinematic distributions in the signal-depleted region show no other significant deviations, the excess is assumed to be a statistical fluctuation.

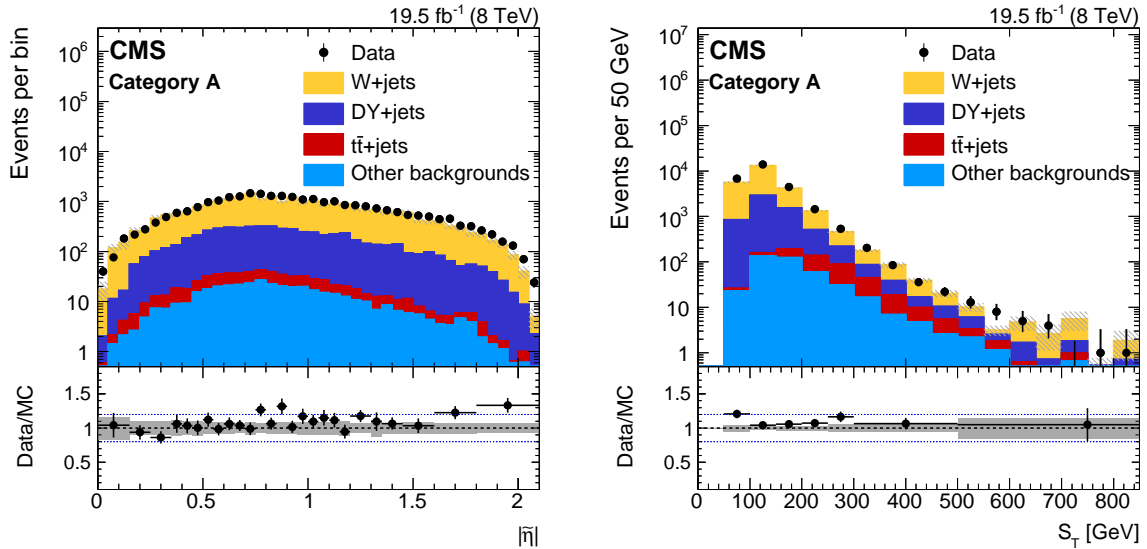


Figure 2: Comparison between data and simulation in the $|\eta|$ (left) and S_T (right) distributions using the signal-depleted selection of events in category A with a same-sign $\mu\tau_h$ pair. Other backgrounds refer to contributions predominantly from processes such as diboson and single top quark production, as well as QCD multijet and other rare SM processes detailed in Section 3. The hatched regions in the distributions and the shaded bands in the Data/MC ratio plots represent the statistical uncertainties in the expectations. The data-simulation agreement is observed to be within 20%, and is assigned as the normalization systematic uncertainty for the $t\bar{t}$ +jets, DY+jets and diboson contributions in the signal region.

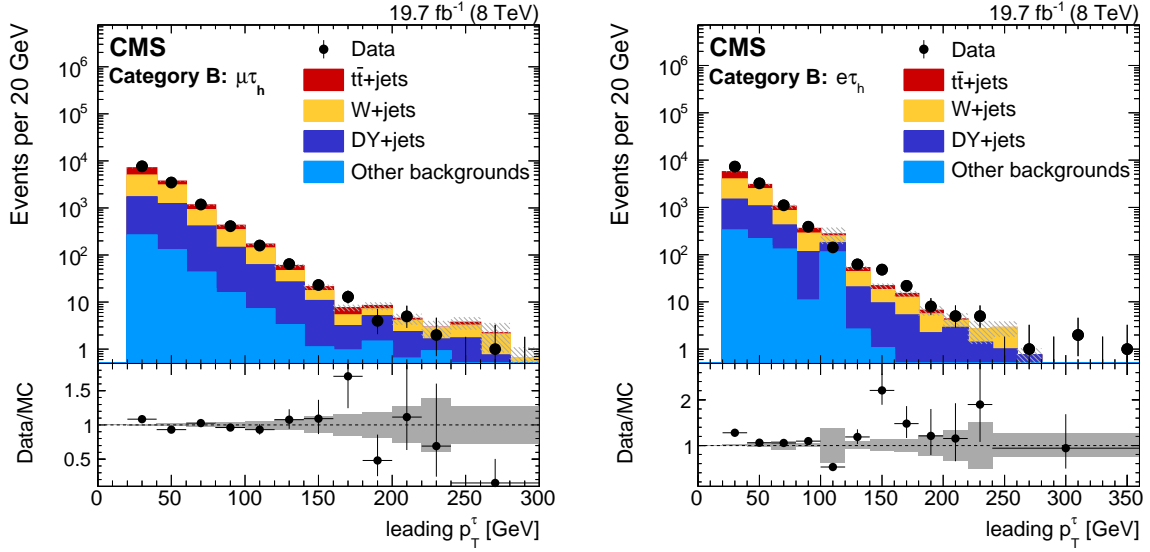


Figure 3: Comparison between data and simulation in the leading τ lepton p_T distributions using the signal-depleted selection of events in category B in the $\mu\tau_h$ channel (left) and in the $e\tau_h$ channel (right). Other backgrounds refer to contributions predominantly from processes such as diboson and single top quark production, but also include QCD multijet and rare SM processes detailed in Section 3. The hatched regions in the distributions and the shaded bands in the Data/MC ratio plots represent the statistical uncertainties in the expectations.

5 Backgrounds

For this analysis, prompt leptons are defined to be those that come from the decays of W bosons, Z bosons or τ leptons, and are usually well isolated. Leptons originating from semileptonic heavy-flavor decays within jets and jets misreconstructed as leptons are both labelled as misidentified leptons, and generally are not isolated. In category A, the expected same-sign background events are mostly due to misidentified leptons, while category B has significant additional prompt-prompt contributions. In accordance with the expected background compositions, data events are used to estimate the dominant misidentified lepton backgrounds in category A, eliminating the need to evaluate the simulation based systematic uncertainties, whereas the prompt-prompt backgrounds in category B require the consideration of these uncertainties. Simulated samples corrected for τ lepton misidentification rates are used for the estimation of the backgrounds in category B.

5.1 Backgrounds in category A

The same-sign dilepton requirement yields a background which mainly consists of events that contain misidentified leptons (especially jets misidentified as τ leptons). These events come from semileptonic $t\bar{t}$ +jets and W +jets processes in approximately equal proportions. Smaller background contributions result from SM processes with genuine same-sign dileptons, such as diboson, $t\bar{t}W$, $t\bar{t}Z$, and $W^\pm W^\pm qq$ events, and opposite-sign dilepton events in which the τ_h charge has been misidentified, such as DY +jets and fully leptonic $t\bar{t}$ +jets events. Events with misidentified leptons contribute up to 90% of the total background, depending on the set of S_T and τ lepton p_T requirements, and are especially dominant in selections for $M_{LQ_3} \leq 400$ GeV.

5.1.1 Lepton misidentification

Background contributions due to misidentified leptons are estimated using the observed data via a “matrix method” [54]. For a given set of selection requirements, four combinations are defined based on the selection quality of the selected same-sign $\mu\tau_h$ pair. Events in which both leptons satisfy the tight selection requirements are classified as TT events, whereas those with both leptons failing the tight selection while satisfying the loose selection requirements are classified as LL events. Similarly, events with only the muon or the τ_h candidate satisfying the tight selection and with the other lepton satisfying the loose selection but failing the tight selection requirements are labeled as TL or LT events, respectively, where the muon is denoted first in the labeling.

The probabilities with which prompt (p) and misidentified (m) muon and τ_h candidates pass a tight selection, given that they satisfy a loose selection, are measured as a function of the lepton p_T in regions of S_T , lepton $|\eta|$, and $\Delta R(\mu, j)_{\min}$ or $\Delta R(\tau, j)_{\min}$. The TT events constitute the search region, whereas TL, LT, and LL events, together with the prompt and misidentification probabilities, are used to calculate the misidentified lepton contributions to the signal region, $N_{\text{TT}}^{\text{misID}}$, as given in Eqs. (2) and (3).

$$\begin{pmatrix} N_{\text{MM}} \\ N_{\text{MP}} \\ N_{\text{PM}} \\ N_{\text{PP}} \end{pmatrix} = \frac{1}{(p_\mu - m_\mu)(p_\tau - m_\tau)} \begin{pmatrix} p_\mu \cdot p_\tau & -p_\mu \cdot \widehat{p}_\tau & -\widehat{p}_\mu \cdot p_\tau & \widehat{p}_\mu \cdot \widehat{p}_\tau \\ -p_\mu \cdot m_\tau & p_\mu \cdot \widehat{m}_\tau & \widehat{p}_\mu \cdot m_\tau & -\widehat{p}_\mu \cdot \widehat{m}_\tau \\ -m_\mu \cdot p_\tau & m_\mu \cdot \widehat{p}_\tau & \widehat{m}_\mu \cdot p_\tau & -\widehat{m}_\mu \cdot \widehat{p}_\tau \\ m_\mu \cdot m_\tau & -m_\mu \cdot \widehat{m}_\tau & -\widehat{m}_\mu \cdot m_\tau & \widehat{m}_\mu \cdot \widehat{m}_\tau \end{pmatrix} \begin{pmatrix} N_{\text{LL}} \\ N_{\text{LT}} \\ N_{\text{TL}} \\ N_{\text{TT}} \end{pmatrix}, \quad (2)$$

$$N_{\text{TT}}^{\text{misID}} = m_\mu m_\tau N_{\text{MM}} + m_\mu p_\tau N_{\text{MP}} + p_\mu m_\tau N_{\text{PM}}. \quad (3)$$

N denotes the number of events in a given combination, and MM, MP, PM, and PP labels denote the double-misidentified, muon misidentified, τ_h misidentified, and double-prompt combinations, respectively. The complementary prompt probability is given as $\widehat{p} = 1 - p$, and the complementary misidentification probability is given as $\widehat{m} = 1 - m$.

Muon and τ lepton prompt probabilities are measured in DY+jets enhanced data regions with $Z \rightarrow \mu\mu$ and $Z \rightarrow \tau\tau \rightarrow \mu\tau_h$ decays, respectively, and in simulated $t\bar{t}$ +jets, W+jets and LQ₃ events. For the τ lepton misidentification probability measurements, a $W(\rightarrow \mu\nu)$ +jets enriched data set with additional τ_h candidates is used. A QCD multijet enhanced data set with a single muon candidate is used for the muon misidentification probability measurements. In simulated samples, the τ lepton misidentification probability measurement is conducted in W+jets, $t\bar{t}$ +jets, and LQ₃ samples, while the muon misidentification probability measurement is made in QCD multijet, $t\bar{t}$ +jets, and LQ₃ samples.

The individual prompt and misidentification probability measurements conducted using simulated samples are combined into a single value for each of the p and m bins. For each of these, an average value and an associated uncertainty is calculated to account for the process dependent variations. These simulation based values are then combined with correction factors derived from the p and m measurements in data, to account for any bias in the simulated detector geometry and response, providing the values used in Eqs. (2) and (3). The resultant muon prompt probabilities vary from $(70 \pm 3)\%$ to $(95 \pm 3)\%$ for low and high p_T muons, whereas τ lepton prompt probabilities are around $(60 \pm 6)\%$. The muon and τ lepton misidentification probabilities are measured to be about $(1 \pm 1)\%$ and $(14 \pm 2)\%$, respectively.

The matrix method yields consistent results for the misidentification backgrounds when applied to a signal-depleted selection of events in data and to simulated events in the signal

region. The expected yields are in agreement with the observations within 1.5 standard deviations in both selections.

5.1.2 Charge misidentification and irreducible backgrounds

The background contributions due to lepton charge misidentification and irreducible processes with same-sign $\mu\tau_h$ pairs are estimated directly from the simulated samples. These prompt-prompt contributions are calculated by requiring a match ($\Delta R < 0.15$) between the reconstructed lepton candidate and a generator-level object of the same kind without any requirement on the charge. The charge misidentification backgrounds are dominated by τ_h candidates, and these backgrounds contribute to 2–3% of the total expected backgrounds in selections for $M_{LQ_3} \leq 400$ GeV, whereas are negligible in those for higher LQ_3 masses.

5.2 Backgrounds in category B

In category B, major background processes are $t\bar{t}$ +jets, W +jets, and DY +jets events. Smaller contributions come from single top quark, diboson, $t\bar{t}Z$, and QCD multijet events. Contributions from prompt-prompt $\ell\tau_h$ pairs are mainly expected in fully leptonic $t\bar{t}$ +jets events, as well as DY +jets events with $Z \rightarrow \tau\tau \rightarrow \ell\tau_h$ decays and diboson events. In all other processes, the τ_h candidates are expected to originate from misidentified jets. The misidentified electron and muon contributions have been found to be negligible after applying isolation and E_T^{miss} requirements. The background estimation in category B is obtained from simulated samples with various corrections applied to account for differences between data and simulation in the reconstruction and identification of misidentified τ lepton candidates.

The τ lepton misidentification rate is defined as the probability for a misidentified τ lepton candidate originating from a jet to satisfy the final τ lepton identification criteria used in the analysis. The corresponding correction factor for the simulation is defined as the ratio of the data and the simulation-based rates. The misidentification rates in data and simulation are measured in $W(\rightarrow \ell\nu)$ +jets enriched events, containing at least one τ lepton candidate. The τ lepton candidate is used as a misidentified probe, and the results are parametrized as a function of the τ lepton p_T . Additional parametrizations, such as S_T , jet multiplicity, and $\Delta R(\tau, j)_{\text{min}}$, reveal no further deviations between the data and simulation. Thus a one-dimensional parametrization as a function of the τ lepton p_T is used to describe any discrepancy between data and simulation. A small discrepancy is observed in the distribution of scale factors as a function of the τ lepton η for $|\eta| > 1.5$. An additional uncertainty is therefore assigned to the τ lepton scale factors for misidentified τ leptons in this η region.

Measurements based on data are corrected by subtracting the small contributions due to prompt τ leptons, muons, and electrons which are misidentified as τ lepton candidates using the predictions from the simulated samples. The systematic uncertainties in the correction factors are estimated by varying the cross sections of the dominant simulated processes within their uncertainties [55].

The resulting correction factors on the τ lepton misidentification rate are found to be in the range of 0.6–1.1 for the four τ lepton p_T regions. These weights are applied to each misidentified τ lepton candidate in all simulated background processes.

A jet originating from gluon emission has a smaller probability of being misidentified as a τ_h candidate than those originating from quarks. Quarks tend to produce incorrectly assigned τ lepton candidates with a like-sign charge. Therefore, an additional systematic uncertainty is assigned to the correction factors based on the flavor composition of jets misidentified as τ leptons. To determine this uncertainty, the measurement of the τ lepton misidentification rate

is repeated for each of the charge combinations of the $\ell\tau_h$ pair, $\tau_h^\pm\ell^\pm$ and $\tau_h^\pm\ell^\mp$. Because of the different production modes of W^+ and W^- bosons at the LHC, the four charge combinations have different quark and gluon compositions. An estimate of the maximally allowed variance in the probability of each quark or gluon type to be misidentified as a τ lepton is obtained via the comparison of the misidentification rate measurements in the four channels. The uncertainties in the misidentification rates are scaled according to the different expected flavor compositions in the signal and $W(\rightarrow \ell\nu)$ +jets enriched regions used for the misidentification rate measurements.

5.3 Systematic uncertainties

In category A, the backgrounds due to misidentified leptons are derived from data and the associated systematic uncertainties are calculated by propagating the uncertainties in the muon and τ lepton prompt and misidentification probability measurements. The uncertainties in the background rate of misidentified leptons lie in the range of 21–28% in the central channel and 21–36% in the forward channel.

In category B, the uncertainties in the correction factors on the misidentification rate of τ leptons vary from 23–38% for the lower three τ lepton p_T regions and up to 58–82% for the highest p_T region in the $\mu\tau_h$ and $e\tau_h$ channels. These uncertainties are propagated to the estimate of the background of misidentified hadronically decaying τ leptons by varying the correction factors applied to the simulation within their uncertainties.

Since both the signal efficiencies and the prompt-prompt contributions to the background in category A and all the signal and background estimates in category B are determined using simulated events, the following sources of systematic uncertainty are considered.

Normalization uncertainties of 20% are applied for $t\bar{t}$ +jets, DY+jets and diboson processes in category A as observed in the signal-depleted region presented in Fig. 2. An uncertainty of 30% is applied for other rare SM process as motivated by the theoretical uncertainties in the NLO cross sections for processes such as $t\bar{t}W$, $t\bar{t}Z$ [46, 47], and triboson [50] production. For category B, these uncertainties in the MC normalization vary in a range between 15% and 100% according to previous measurements [55]. The CMS luminosity used in the normalization of signal and MC samples has an uncertainty of 2.6% [56].

In order to account for uncertainties in the efficiency of τ lepton identification, an uncertainty of 6% is applied for each prompt τ lepton found in the event. The uncertainty in the τ lepton energy is taken into account by varying the energy of all τ leptons by $\pm 3\%$. Uncertainties induced by the energy resolution of prompt τ leptons in simulated samples are estimated by changing the resolution by $\pm 10\%$.

Muon and electron identification, isolation, and trigger efficiencies are determined with a tag-and-probe method [57] in DY+jets enriched data. In both categories, the muon reconstruction and isolation uncertainty is about 1% and the single muon trigger matching uncertainty is $\leq 0.5\%$. Uncertainties in electron identification, isolation, and trigger efficiencies are considered only in the $e\tau_h$ channel of category B. These uncertainties are p_T - and η -dependent and are found to be 0.3% for electrons in the central detector region with $p_T < 50$ GeV and up to 25% for electrons with $p_T > 500$ GeV.

Uncertainties in the jet energy resolution [27] are taken into account by changing the correction factors within their uncertainties. These correction factors lie between 1.05 and 1.29 depending on jet η , with corresponding uncertainties varying from 5% to 16%. The p_T - and η -dependent scale factors for the jet energy scale [27] are similarly varied by one standard deviation to obtain

the corresponding uncertainties in simulated samples. This corresponds to a 1–3% variation of the scale factors.

The energy scale and resolution uncertainties in τ lepton, muon, electron, and jet candidates are also propagated in the calculation of E_T^{miss} and S_T .

The uncertainty in the pileup re-weighting of simulated samples is estimated by varying the total inelastic cross section [58] by 5%. Signal samples are produced with the CTEQ6L1 PDF set and the associated PDF uncertainties in the signal acceptance are estimated using the PDF uncertainty prescription for LHC [59–61]. In category B, the PDF uncertainties are also calculated for the background processes estimated using simulations.

Additional uncertainties in major SM processes estimated from simulations are considered in category B. Uncertainties in the factorization and normalization scales, μ_r and μ_f , respectively, on $t\bar{t}$ +jets and W +jets events are calculated by changing the corresponding scales by a factor of 2 or 0.5. The effect of an uncertainty in the jet-parton matching threshold in the simulation of W +jets processes is evaluated by varying it within a factor of 2. The uncertainty in the top quark p_T re-weighting procedure is estimated by doubling and removing the correction factors.

Table 2 shows a summary of the systematic uncertainties for categories A and B.

Table 2: Systematic uncertainty sources and their effects on background (B) and signal (S) estimates. Uncertainties affecting the signal yields in both categories and the background yields in category A are calculated using the selection criteria for the $M_{LQ_3} = 550$ GeV hypothesis. In category A, the uncertainties are reported for central/forward channels separately, where appropriate. In category B, all uncertainties are averaged over the four p_T^τ search bins. All values are symmetric except for the PDF uncertainty in the signal acceptance in category A, and the $t\bar{t}$ factorization and normalization scale uncertainty in category B. The τ misidentification rate uncertainties considered in category B are included in the matrix method uncertainty in category A. All uncertainties in the background estimates are scaled according to their relative contributions to the total expected background.

Systematic uncertainty	Magnitude (%)	Category A		Category B			
		B (%)	S (%)	$\mu\tau_h$ ch.		$e\tau_h$ ch.	
		B (%)	S (%)	B (%)	S (%)	B (%)	S (%)
Integrated luminosity	2.6	0.4/1.2	2.6	2.6	2.6	2.6	2.6
Electron reco/ID/iso & trigger	p_T, η dependent	—	—	—	—	1.4	2.2
Muon reco/ID/iso & trigger	1.1	0.1/0.5	1.1	0.9	0.9	—	—
τ lepton reco/ID/iso	6.0	0.8/2.8	6.0	1.5	3.0	0.6	3.1
Muon momentum scale & resolution	p_T dependent	0.1/0.3	0.4	—	—	—	—
τ lepton energy scale	3.0	1.2/4.1	2.0	2.3	2.7	0.6	1.5
τ lepton energy resolution	10.0	0.2/0.8	0.9	1.2	1.3	0.2	0.1
Jet energy scale	p_T, η dependent	0.9/3.2	1.9	4.2	1.9	5.6	2.7
Jet energy resolution	η dependent	0.4/1.2	1.0	0.8	0.3	1.6	0.8
Pileup	5.0	0.1/1.2	1.0/2.5	0.8	0.3	0.9	0.5
PDF (on acceptance)	—	—	$+2.9/+2.4$ $-4.3/-6.2$	—	0.7	—	0.9
PDF (on background)	—	—	—	8.7	—	8.3	—
Matrix method	—	23.1/15.3	—	—	—	—	—
Jet $\rightarrow \tau$ misidentification rate	p_T dependent	—	—	8.2	1.0	10.9	0.8
$e \rightarrow \tau$ misidentification rate	η dependent	—	—	0.1	0.1	0.1	0.1
$t\bar{t}$ factorization/renormalization	$+100$ -50	—	—	$+6.1$ -5.9	—	$+2.9$ -2.7	—
Top quark p_T re-weighting	p_T dependent	—	—	0.1	—	0.1	—
W +jets factorization/renormalization	$+100$ -50	—	—	4.3	—	0.3	—
W +jets matching threshold	$+100$ -50	—	—	1.3	—	2.5	—

6 Results

The search results for category A (B) are presented in Table 3 (4 and 5). Figures 4 and 5 show the comparison of data and the predicted backgrounds as a function of S_T , τ lepton p_T , and jet multiplicity parameters. The dashed curves show the expectation for LQ signals. For the comparison of expected and observed number of events in Tables 3–5 and Figs. 4–5, Z -scores are used. These are computed taking into account the total uncertainty in the mean number of expected events. A unit Z -score, $|Z| = 1$, refers to a two-tailed 1-standard deviation quantile ($\sim 68\%$) of the normal distribution. For each selection, the observed number of events is found to be in an overall agreement with the SM-only hypothesis and the distributions reveal no statistically significant deviations from the SM expectations.

A limit is set on the pair production cross section of charge $-1/3$ third-generation scalar LQs by using a combined likelihood fit in the ten search regions of category A and B. The theta tool [62] is used to produce Bayesian limits on the signal cross section, where the statistical and systematic uncertainties are treated as nuisance parameters. Statistical and systematic uncertainties that are specific to category A or B, such as the uncertainties in the backgrounds from misidentified leptons, are assumed to be uncorrelated, whereas common sources of systematic uncertainties are treated as fully correlated. The common uncertainties are the uncertainties in the jet energy scale and resolution, τ lepton and muon identification and isolation efficiencies, τ lepton energy scale and resolution, PDFs, and integrated luminosity.

The observed and expected exclusion limits as a function of the LQ mass are shown in Fig. 6. Assuming a unit branching fraction of LQ decays to top quark and τ lepton pairs, pair production of third-generation LQs is excluded for masses up to 685 GeV with an expected limit of 695 GeV. The exclusion limits worsen as the LQ_3 mass approaches the mass of the top quark because the LQ_3 decay products become softer. At $M_{LQ_3} = 200$ GeV, more than 90% of τ leptons originating from LQ_3 decays have $p_T < 60$ GeV, which causes a decrease both in the signal selection efficiency and the discriminating performance of the τ lepton p_T spectrum. Therefore, no exclusion limits are quoted for masses below 200 GeV.

Branching fraction dependent exclusion limits are presented in Fig. 6 (lower right), where limits on the complementary $LQ_3 \rightarrow b\nu$ ($\beta = 0$) decay channel are also included. The results for $\beta = 0$ are obtained via reinterpretation of a search for pair produced bottom squarks [17] with subsequent decays into b quark and neutralino pairs, in the limit of vanishing neutralino masses. In a statistical combination of this analysis with the search for bottom squarks, third-generation scalar LQs are also excluded for masses below 700 GeV for $\beta = 0$ and for masses below 560 GeV over the full β range. If upper limits on β are to be used to constrain the lepton-quark-LQ Yukawa couplings, $\lambda_{b\nu}$ and $\lambda_{\tau\tau}$, kinematic suppression factors that favor $b\nu$ decay over the $\tau\tau$ have to be considered as well as the relative strengths of the two Yukawa couplings [12, 13].

Additionally, the results presented here for the third-generation scalar LQs are directly reinterpreted in the context of pair produced bottom squarks decaying into top quark and τ lepton pairs. Thus, pair production of bottom squarks where the decay mode is dominated by the RPV coupling λ'_{333} is also excluded up to a bottom squark mass of 685 GeV.

Table 3: Category A search results in the signal region for several LQ_3 mass hypotheses. The τ lepton p_T and S_T columns represent the optimized thresholds defined in Section 4.1. The corresponding expected number of prompt-prompt and total background events, as well as the observed number of data events are listed as $N_{\text{Bkg}}^{\text{PP}}$, total $N_{\text{Bkg}}^{\text{Exp}}$, and N^{Obs} . The statistical and systematic uncertainties quoted in the expected number of background events are combinations of misidentified lepton and prompt-prompt components. The ϵ_{LQ_3} is the expected signal efficiency at a given LQ_3 mass with respect to the total number of expected LQ_3 signal events at $\sqrt{s} = 8$ TeV with a $\mu\tau_h$ pair of any charge combination. No expected signal efficiency for $M_{LQ_3} = 200$ GeV is reported in the forward channel since the associated yield in the signal sample was measured to be zero.

M_{LQ_3} (GeV)	p_T^τ (GeV)	S_T (GeV)	$N_{\text{Bkg}}^{\text{PP}}$ \pm (stat)	Total $N_{\text{Bkg}}^{\text{Exp}}$ \pm (stat) \pm (syst)	N^{Obs}	Z-score	$N_{LQ_3}^{\text{Exp}}$ \pm (stat)	ϵ_{LQ_3} (%)
Central channel: $ \widetilde{\eta} < 0.9$								
200	35	410	8.5 ± 1.0	$128 \pm 5 \pm 25$	105	-1.0	53 ± 21	0.04
250	35	410	8.5 ± 1.0	$128 \pm 5 \pm 25$	105	-1.0	252 ± 24	0.58
300	50	470	4.2 ± 0.5	$39.9 \pm 2.9 \pm 8.3$	27	-1.5	153 ± 11	0.98
350	50	490	4.0 ± 0.5	$34.6 \pm 2.7 \pm 7.1$	25	-1.2	92.4 ± 5.6	1.45
400	65	680	0.9 ± 0.2	$7.2 \pm 1.2 \pm 1.7$	4	-1.0	28.4 ± 2.1	1.00
450	65	700	0.8 ± 0.2	$6.3 \pm 1.1 \pm 1.6$	4	-0.8	17.3 ± 1.1	1.27
500	65	770	0.5 ± 0.2	$3.2 \pm 0.8 \pm 0.8$	4	+0.5	9.8 ± 0.6	1.43
550	65	800	0.4 ± 0.1	$2.7 \pm 0.8 \pm 0.6$	4	+0.7	6.1 ± 0.3	1.71
600	65	850	0.2 ± 0.1	$1.8 \pm 0.6 \pm 0.4$	3	+0.9	3.6 ± 0.2	1.85
650	65	850	0.2 ± 0.1	$1.8 \pm 0.6 \pm 0.4$	3	+0.9	2.2 ± 0.1	1.99
700	85	850	0.1 ± 0.1	$1.1 \pm 0.5 \pm 0.3$	2	+0.8	1.3 ± 0.1	2.02
750	85	850	0.1 ± 0.1	$1.1 \pm 0.5 \pm 0.3$	2	+0.8	0.8 ± 0.1	2.20
800	85	850	0.1 ± 0.1	$1.1 \pm 0.5 \pm 0.3$	2	+0.8	0.5 ± 0.1	2.80
Forward channel: $ \widetilde{\eta} \geq 0.9$								
200	35	410	4.2 ± 0.5	$72 \pm 4 \pm 15$	87	+1.1	—	—
250	35	410	4.2 ± 0.5	$72 \pm 4 \pm 15$	87	+1.1	50 ± 11	0.11
300	50	470	1.8 ± 0.3	$20.3 \pm 2.2 \pm 3.9$	23	+0.5	33.4 ± 5.2	0.21
350	50	490	1.7 ± 0.3	$18.2 \pm 2.0 \pm 3.5$	19	+0.2	18.5 ± 2.5	0.29
400	65	680	0.7 ± 0.2	$2.7 \pm 0.7 \pm 0.6$	1	-0.9	6.1 ± 1.0	0.21
450	65	700	0.7 ± 0.2	$2.3 \pm 0.6 \pm 0.4$	1	-0.7	3.8 ± 0.5	0.28
500	65	770	0.5 ± 0.1	$1.2 \pm 0.4 \pm 0.2$	1	0.0	1.6 ± 0.2	0.24
550	65	800	0.4 ± 0.1	$0.9 \pm 0.4 \pm 0.2$	1	+0.3	1.2 ± 0.2	0.32
600	65	850	0.3 ± 0.1	$0.6 \pm 0.3 \pm 0.1$	1	+0.6	0.6 ± 0.1	0.29
650	65	850	0.3 ± 0.1	$0.6 \pm 0.3 \pm 0.1$	1	+0.6	0.3 ± 0.1	0.26
700	85	850	0.1 ± 0.1	$0.4 \pm 0.2 \pm 0.1$	0	-0.4	0.2 ± 0.1	0.28
750	85	850	0.1 ± 0.1	$0.4 \pm 0.2 \pm 0.1$	0	-0.4	0.1 ± 0.1	0.35
800	85	850	0.1 ± 0.1	$0.4 \pm 0.2 \pm 0.1$	0	-0.4	0.1 ± 0.1	0.36

Table 4: Category B search results for the four p_T^τ search regions of the $\mu\tau_h$ channel. All expected values for background and signal processes (LQ₃ masses indicated in parentheses) are reported with the corresponding statistical and systematic uncertainties. The expected signal efficiency ϵ_{LQ_3} at a given LQ₃ mass is determined with respect to the total number of expected LQ₃ signal events at $\sqrt{s} = 8$ TeV with a $\mu\tau_h$ pair of any charge combination, and ϵ_{LQ_3} is reported separately for opposite-sign (OS) and same-sign (SS) $\mu\tau_h$ events.

Process	$p_T^\tau < 60$ GeV	$60 < p_T^\tau < 120$ GeV	$120 < p_T^\tau < 200$ GeV	$p_T^\tau > 200$ GeV	ϵ_{LQ_3} (%)	
					OS	SS
LQ ₃ (200 GeV)	$21 \pm 12_{-2}^{+7}$	$0.0 \pm 0.1 \pm 0.0$	$0.0 \pm 0.1 \pm 0.1$	$0.0 \pm 0.1 \pm 0.1$	0.01	0
LQ ₃ (250 GeV)	$31.0 \pm 8.2_{-3.4}^{+6.6}$	$13.1 \pm 5.5_{-2.9}^{+1.1}$	$0.0 \pm 0.1 \pm 0.1$	$0.0 \pm 0.1 \pm 0.1$	0.09	0.02
LQ ₃ (300 GeV)	$33.1 \pm 5.3_{-3.8}^{+2.8}$	$24.6 \pm 4.6_{-2.1}^{+2.8}$	$7.6 \pm 2.6_{-1.7}^{+1.1}$	$3.9 \pm 1.8_{-0.3}^{+0.9}$	0.35	0.08
LQ ₃ (350 GeV)	$18.1 \pm 2.6_{-1.4}^{+1.8}$	$13.3 \pm 2.2_{-1.1}^{+1.0}$	$7.2 \pm 1.6_{-0.7}^{+0.8}$	$2.9 \pm 0.9_{-1.4}^{+0.5}$	0.57	0.08
LQ ₃ (400 GeV)	$13.9 \pm 1.4_{-2.6}^{+1.1}$	$13.4 \pm 1.4_{-1.1}^{+1.0}$	$7.8 \pm 1.1_{-0.6}^{+0.8}$	$4.1 \pm 0.8_{-0.8}^{+0.6}$	1.30	0.12
LQ ₃ (450 GeV)	$10.1 \pm 0.9_{-1.9}^{+0.8}$	$8.6 \pm 0.8_{-0.8}^{+0.8}$	$7.1 \pm 0.7_{-0.6}^{+0.5}$	$5.8 \pm 0.6_{-0.6}^{+0.7}$	2.05	0.27
LQ ₃ (500 GeV)	$5.2 \pm 0.4_{-0.9}^{+0.5}$	$6.0 \pm 0.5 \pm 0.5$	$5.3 \pm 0.4_{-0.5}^{+0.4}$	$4.4 \pm 0.4_{-0.5}^{+0.7}$	2.75	0.27
LQ ₃ (550 GeV)	$3.2 \pm 0.3_{-0.6}^{+0.3}$	$4.4 \pm 0.3_{-0.3}^{+0.4}$	$4.3 \pm 0.3_{-0.4}^{+0.5}$	$4.0 \pm 0.3 \pm 0.4$	4.04	0.36
LQ ₃ (600 GeV)	$2.0 \pm 0.1_{-0.5}^{+0.2}$	$2.7 \pm 0.2 \pm 0.2$	$2.7 \pm 0.2 \pm 0.2$	$3.5 \pm 0.2 \pm 0.4$	5.11	0.43
LQ ₃ (650 GeV)	$1.3 \pm 0.1_{-0.3}^{+0.1}$	$1.8 \pm 0.1_{-0.2}^{+0.1}$	$2.0 \pm 0.1 \pm 0.2$	$2.5 \pm 0.1_{-0.2}^{+0.3}$	6.07	0.67
LQ ₃ (700 GeV)	$0.7 \pm 0.1 \pm 0.1$	$1.1 \pm 0.1 \pm 0.1$	$1.1 \pm 0.1 \pm 0.1$	$1.6 \pm 0.1_{-0.1}^{+0.2}$	6.66	0.57
LQ ₃ (750 GeV)	$0.4 \pm 0.1 \pm 0.1$	$0.5 \pm 0.1 \pm 0.1$	$0.7 \pm 0.1 \pm 0.1$	$1.1 \pm 0.1 \pm 0.1$	6.71	0.59
LQ ₃ (800 GeV)	$0.2 \pm 0.1 \pm 0.1$	$0.4 \pm 0.1 \pm 0.1$	$0.5 \pm 0.1 \pm 0.1$	$0.8 \pm 0.1 \pm 0.1$	7.77	0.61
$t\bar{t}$ +jets	$29.9 \pm 2.9_{-7.2}^{+7.3}$	$8.8 \pm 1.3_{-3.4}^{+3.2}$	$1.7 \pm 0.6_{-0.6}^{+0.6}$	$0.4 \pm 0.3_{-0.4}^{+0.9}$		
W+jets	$7.4 \pm 1.7_{-5.1}^{+5.1}$	$0.6 \pm 0.5 \pm 0.6$	$0.0 \pm 0.1 \pm 0.1$	$0.4 \pm 0.4 \pm 0.4$		
DY+jets	$4.8 \pm 0.7 \pm 2.5$	$1.8 \pm 0.4_{-0.9}^{+1.1}$	$0.5 \pm 0.2 \pm 0.3$	$0.4 \pm 0.2 \pm 0.2$		
Other backgrounds	$3.1 \pm 0.9_{-1.9}^{+1.8}$	$0.2 \pm 0.1_{-0.3}^{+0.8}$	$0.2 \pm 0.1 \pm 0.4$	$0.1 \pm 0.1_{-0.2}^{+0.1}$		
Total $N_{\text{Bkg}}^{\text{Exp}}$	$45.2 \pm 3.5_{-9.3}^{+9.4}$	$11.5 \pm 1.4_{-3.6}^{+3.4}$	$2.5 \pm 0.6 \pm 0.8$	$1.2 \pm 0.5_{-0.6}^{+1.0}$		
N^{Obs}	44	15	1	0		
Z-score	-0.1	+0.7	+0.8	-1.0		

Table 5: Category B search results for the four p_T^τ search regions of the $e\tau_h$ channel. All expected values for background and signal processes (LQ₃ masses indicated in parentheses) are reported with the corresponding statistical and systematic uncertainties. The expected signal efficiency ϵ_{LQ_3} at a given LQ₃ mass is determined with respect to the total number of expected LQ₃ signal events at $\sqrt{s} = 8$ TeV with an $e\tau_h$ pair of any charge combination.

Process	$p_T^\tau < 60$ GeV	$60 < p_T^\tau < 120$ GeV	$120 < p_T^\tau < 200$ GeV	$p_T^\tau > 200$ GeV	ϵ_{LQ_3}
LQ ₃ (200 GeV)	$32 \pm 19^{+6}_{-4}$	$0.1 \pm 0.1 \pm 0.1$	$0.0 \pm 0.1 \pm 0.1$	$0.0 \pm 0.1 \pm 0.1$	0.02
LQ ₃ (250 GeV)	$33.3 \pm 8.7^{+8.2}_{-5.8}$	$11.9 \pm 5.3^{+2.6}_{-2.4}$	$0.0 \pm 0.1 \pm 0.1$	$0.0 \pm 0.1 \pm 0.1$	0.16
LQ ₃ (300 GeV)	$31.9 \pm 5.2^{+3.2}_{-9.1}$	$27.7 \pm 4.6^{+3.9}_{-4.4}$	$4.2 \pm 1.9^{+1.1}_{-0.3}$	$2.7 \pm 1.6^{+0.2}_{-0.3}$	0.70
LQ ₃ (350 GeV)	$19.6 \pm 2.6^{+2.7}_{-3.6}$	$19.6 \pm 2.5^{+2.0}_{-2.1}$	$8.6 \pm 1.7^{+1.4}_{-0.8}$	$4.7 \pm 1.3 \pm 0.5$	1.35
LQ ₃ (400 GeV)	$12.7 \pm 1.4^{+1.7}_{-2.6}$	$14.6 \pm 1.5^{+2.0}_{-1.4}$	$8.1 \pm 1.1^{+1.2}_{-1.3}$	$4.8 \pm 0.9^{+0.6}_{-0.4}$	2.22
LQ ₃ (450 GeV)	$7.8 \pm 0.7^{+1.3}_{-1.4}$	$10.1 \pm 0.9^{+0.9}_{-1.1}$	$7.2 \pm 0.7^{+1.0}_{-0.7}$	$5.5 \pm 0.6^{+0.6}_{-0.8}$	3.65
LQ ₃ (500 GeV)	$4.8 \pm 0.4^{+0.5}_{-1.2}$	$7.3 \pm 0.5^{+0.8}_{-0.9}$	$5.5 \pm 0.4 \pm 0.6$	$5.2 \pm 0.4^{+0.7}_{-0.6}$	5.34
LQ ₃ (550 GeV)	$3.3 \pm 0.2^{+0.4}_{-1.0}$	$4.3 \pm 0.3 \pm 0.4$	$4.4 \pm 0.3 \pm 0.4$	$4.3 \pm 0.3 \pm 0.5$	7.28
LQ ₃ (600 GeV)	$1.9 \pm 0.1^{+0.2}_{-0.6}$	$2.9 \pm 0.2 \pm 0.3$	$3.2 \pm 0.2 \pm 0.3$	$3.6 \pm 0.2 \pm 0.4$	9.61
LQ ₃ (650 GeV)	$1.2 \pm 0.1^{+0.1}_{-0.4}$	$1.8 \pm 0.1 \pm 0.2$	$2.0 \pm 0.1 \pm 0.2$	$2.4 \pm 0.1^{+0.3}_{-0.3}$	10.89
LQ ₃ (700 GeV)	$0.7 \pm 0.1^{+0.1}_{-0.2}$	$1.1 \pm 0.1 \pm 0.1$	$1.5 \pm 0.1 \pm 0.1$	$1.9 \pm 0.1 \pm 0.2$	13.11
LQ ₃ (750 GeV)	$0.4 \pm 0.1 \pm 0.1$	$0.7 \pm 0.1 \pm 0.1$	$0.7 \pm 0.1 \pm 0.1$	$1.4 \pm 0.1^{+0.1}_{-0.2}$	13.84
LQ ₃ (800 GeV)	$0.2 \pm 0.1 \pm 0.1$	$0.4 \pm 0.1 \pm 0.1$	$0.5 \pm 0.1 \pm 0.1$	$0.9 \pm 0.1 \pm 0.1$	14.82
$t\bar{t}$ +jets	$27.7 \pm 2.4 \pm 7.7$	$7.5 \pm 1.2^{+2.1}_{-2.8}$	$0.9 \pm 0.4 \pm 0.3$	$0.1 \pm 0.1^{+0.6}_{-0.1}$	
W+jets	$8.5 \pm 1.8^{+5.3}_{-5.4}$	$1.1 \pm 0.6^{+0.6}_{-0.7}$	$0.0 \pm 0.1 \pm 0.1$	$0.0 \pm 0.1 \pm 0.1$	
DY+jets	$4.4 \pm 0.7^{+2.3}_{-2.4}$	$1.4 \pm 0.4^{+0.8}_{-0.7}$	$0.6 \pm 0.2 \pm 0.3$	$0.2 \pm 0.1 \pm 0.1$	
Other backgrounds	$3.5 \pm 1.0^{+2.5}_{-3.0}$	$1.1 \pm 0.5^{+0.7}_{-0.8}$	$0.2 \pm 0.1 \pm 0.2$	$0.4 \pm 0.3 \pm 0.2$	
Total $N_{\text{Bkg}}^{\text{Exp}}$	$44.1 \pm 3.2^{+10.0}_{-10.1}$	$11.0 \pm 1.5^{+2.5}_{-3.1}$	$1.6 \pm 0.5 \pm 0.5$	$0.7 \pm 0.4^{+0.7}_{-0.3}$	
N^{Obs}	53	5	4	1	
Z-score	+0.8	-1.2	+1.1	+0.1	

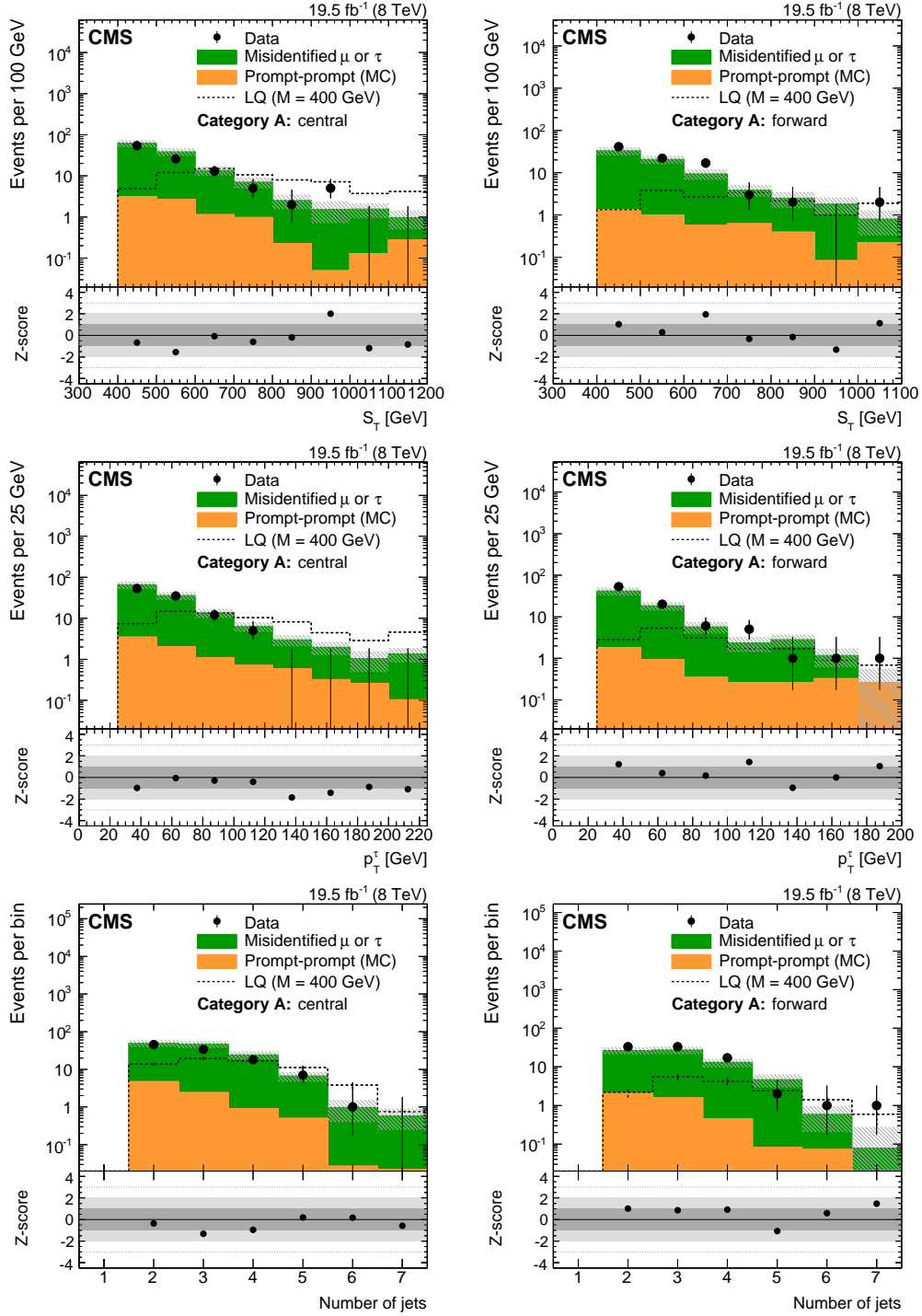


Figure 4: The S_T , τ lepton p_T , and jet multiplicity distributions in the signal region of category A for central (left column) and forward (right column) channels, using the optimized selection for $M_{LQ_3} = 200$ GeV (all other optimized selection criteria yield events that are a subset of this selection). The rightmost bin of each distribution includes overflow and no statistically significant excess is observed in the suppressed bins. The systematic uncertainty for each bin of these distributions is determined independently. Shaded regions in the histograms represent the total statistical and systematic uncertainty in the background expectation. The Z-score distribution is provided at the bottom of each plot.

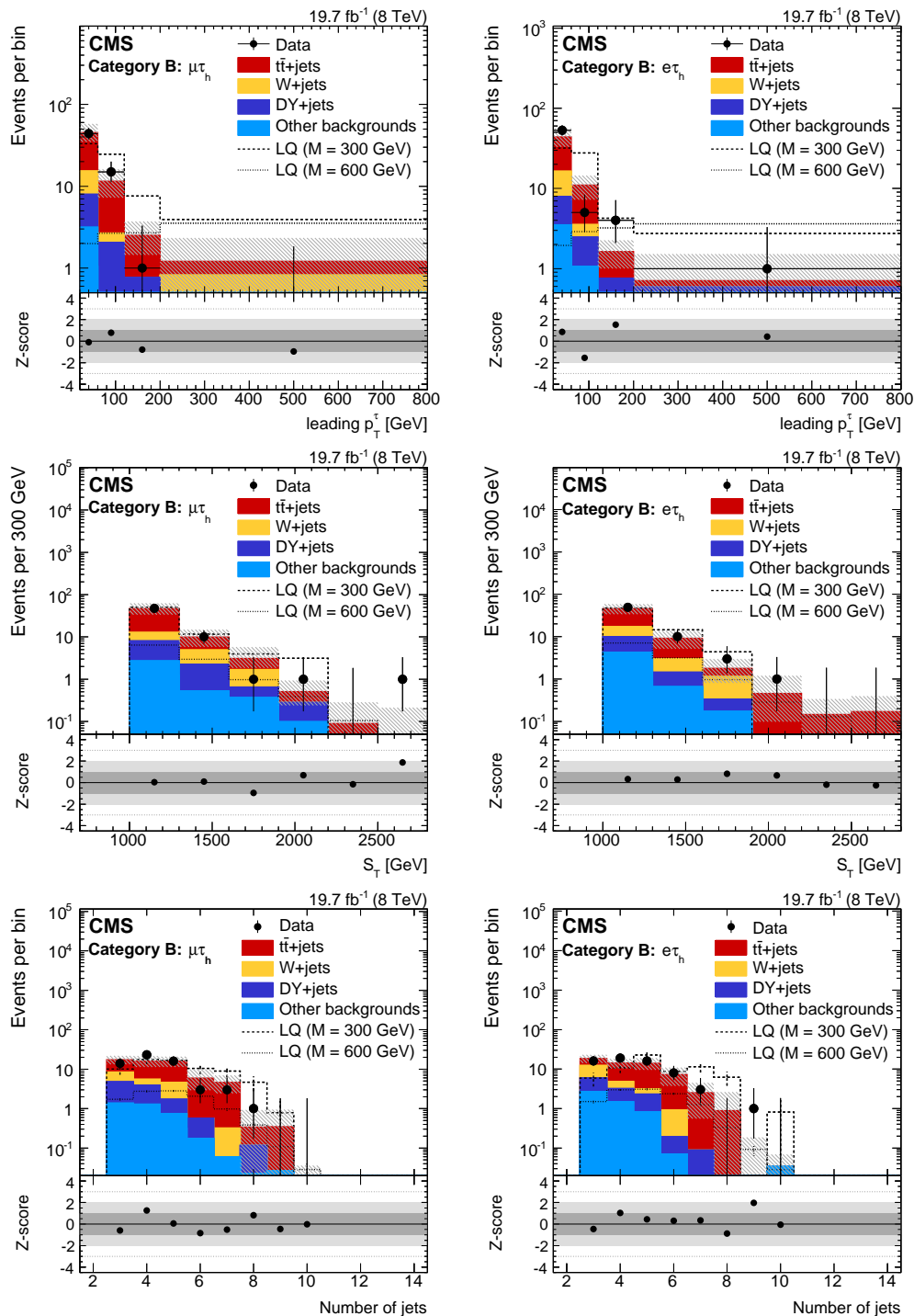


Figure 5: The leading τ lepton p_T , S_T , and jet multiplicity distributions in the signal region of category B for $\mu\tau_h$ (left column) and $e\tau_h$ (right column) channels. The rightmost bin of each distribution includes overflow and no statistically significant excess is observed in the suppressed bins. Shaded regions in the histograms represent the total statistical and systematic uncertainty in the background expectation. The Z-score distribution is provided at the bottom of each plot. The four regions of the τ lepton p_T correspond to the four search regions.

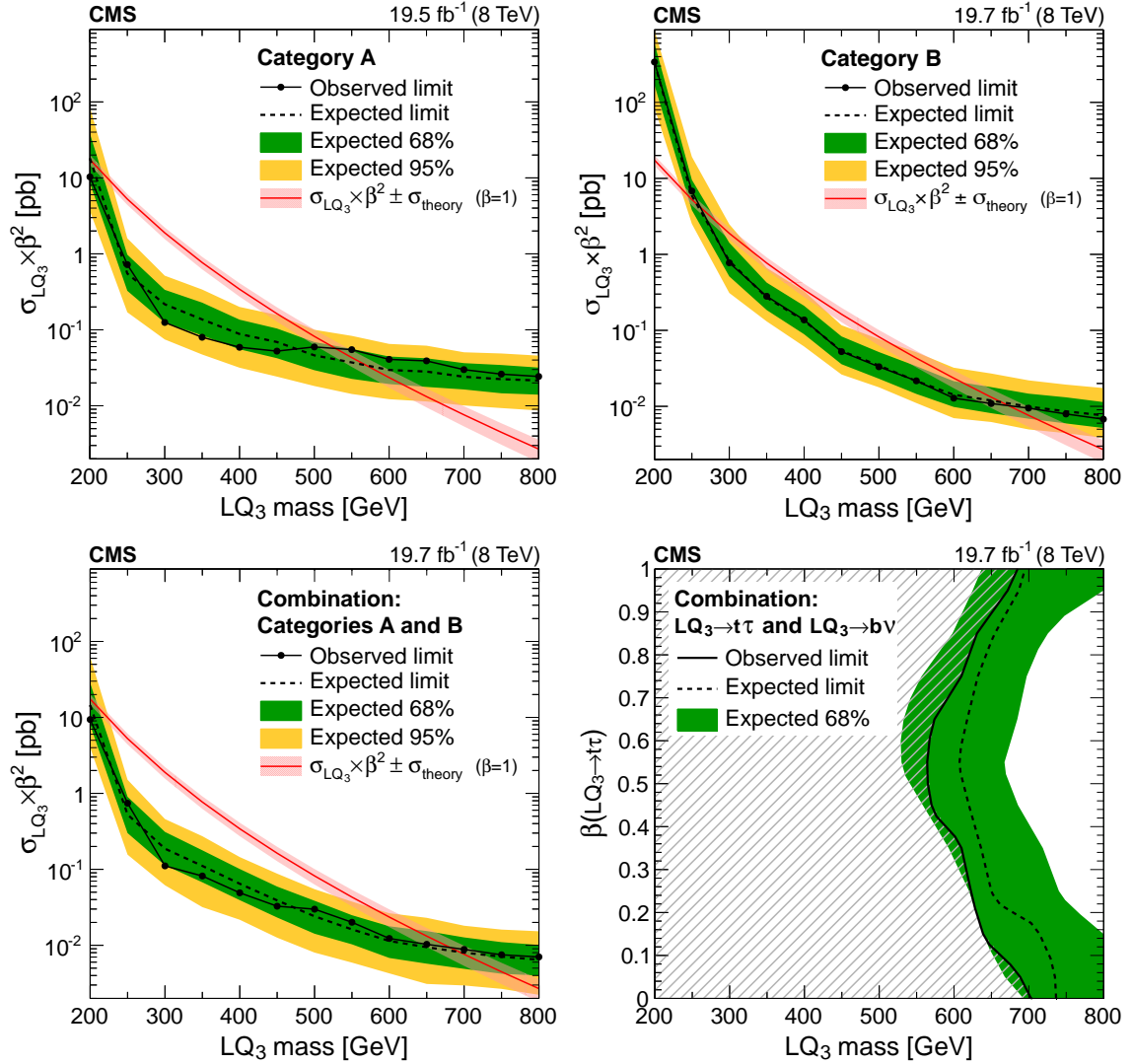


Figure 6: The expected and observed exclusion limits at 95% CL on the LQ₃ pair production cross section times β^2 in category A (upper left), category B (upper right) and the combination of the two categories (lower left). The theoretical uncertainty in the LQ pair production cross section includes the PDF and renormalization/factorization scale uncertainties as prescribed in Ref. [19]. The expected and observed limits on the LQ branching fraction β as a function of the LQ mass (lower right). The total excluded region (shaded) is obtained by including the results in Ref. [17], reinterpreted for the LQ₃ → b ν scenario.

7 Summary

A search for pair produced, charge $-1/3$, third-generation scalar leptoquarks decaying to top quark and τ lepton pairs has been conducted in the $\ell\tau_h$ channel with two or more jets, using a proton-proton collisions data sample collected with the CMS detector at $\sqrt{s} = 8$ TeV corresponding to an integrated luminosity of 19.7 fb^{-1} . No statistically significant excess is observed over the SM background expectations. Assuming that all leptoquarks decay to a top quark and a τ lepton, the pair production of charge $-1/3$, third-generation scalar leptoquarks is excluded at 95% CL for masses up to 685 GeV (695 GeV expected). This constitutes the first direct result for leptoquarks decaying in this channel, and the mass limit is also directly applicable to pair produced bottom squarks decaying via the RPV coupling λ'_{333} .

Acknowledgments

We congratulate our colleagues in the CERN accelerator departments for the excellent performance of the LHC and thank the technical and administrative staffs at CERN and at other CMS institutes for their contributions to the success of the CMS effort. In addition, we gratefully acknowledge the computing centers and personnel of the Worldwide LHC Computing Grid for delivering so effectively the computing infrastructure essential to our analyses. Finally, we acknowledge the enduring support for the construction and operation of the LHC and the CMS detector provided by the following funding agencies: BMWFW and FWF (Austria); FNRS and FWO (Belgium); CNPq, CAPES, FAPERJ, and FAPESP (Brazil); MES (Bulgaria); CERN; CAS, MoST, and NSFC (China); COLCIENCIAS (Colombia); MSES and CSF (Croatia); RPF (Cyprus); MoER, ERC IUT and ERDF (Estonia); Academy of Finland, MEC, and HIP (Finland); CEA and CNRS/IN2P3 (France); BMBF, DFG, and HGF (Germany); GSRT (Greece); OTKA and NIH (Hungary); DAE and DST (India); IPM (Iran); SFI (Ireland); INFN (Italy); MSIP and NRF (Republic of Korea); LAS (Lithuania); MOE and UM (Malaysia); CINVESTAV, CONACYT, SEP, and UASLP-FAI (Mexico); MBIE (New Zealand); PAEC (Pakistan); MSHE and NSC (Poland); FCT (Portugal); JINR (Dubna); MON, RosAtom, RAS and RFBR (Russia); MESTD (Serbia); SEIDI and CPAN (Spain); Swiss Funding Agencies (Switzerland); MST (Taipei); ThEPCenter, IPST, STAR and NSTDA (Thailand); TUBITAK and TAEK (Turkey); NASU and SFFR (Ukraine); STFC (United Kingdom); DOE and NSF (USA).

Individuals have received support from the Marie-Curie program and the European Research Council and EPLANET (European Union); the Leventis Foundation; the A. P. Sloan Foundation; the Alexander von Humboldt Foundation; the Belgian Federal Science Policy Office; the Fonds pour la Formation à la Recherche dans l'Industrie et dans l'Agriculture (FRIA-Belgium); the Agentschap voor Innovatie door Wetenschap en Technologie (IWT-Belgium); the Ministry of Education, Youth and Sports (MEYS) of the Czech Republic; the Council of Science and Industrial Research, India; the HOMING PLUS program of the Foundation for Polish Science, cofinanced from European Union, Regional Development Fund; the Compagnia di San Paolo (Torino); the Consorzio per la Fisica (Trieste); MIUR project 20108T4XTM (Italy); the Thalís and Aristeia programs cofinanced by EU-ESF and the Greek NSRF; and the National Priorities Research Program by Qatar National Research Fund.

References

- [1] “Lepton number as the fourth “color”, doi:10.1103/PhysRevD.10.275. [Erratum: doi:10.1103/PhysRevD.11.703.2].

- [2] H. Georgi and S. L. Glashow, “Unity of All Elementary Particle Forces”, *Phys. Rev. Lett.* **32** (1974) 438, doi:10.1103/PhysRevLett.32.438.
- [3] S. Chakdar, T. Li, S. Nandi, and S. K. Rai, “Unity of elementary particles and forces for the third family”, *Phys. Lett. B* **718** (2012) 121, doi:10.1016/j.physletb.2012.10.021, arXiv:1206.0409.
- [4] E. Farhi and L. Susskind, “Technicolor”, *Phys. Rept.* **74** (1981) 277, doi:10.1016/0370-1573(81)90173-3.
- [5] B. Schrempp and F. Schrempp, “Light leptoquarks”, *Phys. Lett. B* **153** (1985) 101, doi:10.1016/0370-2693(85)91450-9.
- [6] B. Gripaios, “Composite leptoquarks at the LHC”, *JHEP* **02** (2010) 045, doi:10.1007/JHEP02(2010)045, arXiv:0910.1789.
- [7] W. Buchmüller, R. Rückl, and D. Wyler, “Leptoquarks in lepton-quark collisions”, *Phys. Lett. B* **191** (1987) 442, doi:10.1016/0370-2693(87)90637-X. [Erratum: doi:10.1016/S0370-2693(99)00014-3].
- [8] D. E. Acosta and S. K. Blessing, “Leptoquark Searches at HERA and the Tevatron”, *Ann. Rev. Nucl. Part. Sci.* **49** (1999) 389, doi:10.1146/annurev.nucl.49.1.389.
- [9] ATLAS Collaboration, “Search for first generation scalar leptoquarks in pp collisions at $\sqrt{s} = 7$ TeV with the ATLAS detector”, *Phys. Lett. B* **709** (2012) 158, doi:10.1016/j.physletb.2012.02.004, arXiv:1112.4828. [Erratum: doi:10.1016/j.physletb.2012.03.023].
- [10] ATLAS Collaboration, “Search for second generation scalar leptoquarks in pp collisions at $\sqrt{s} = 7$ TeV with the ATLAS detector”, *Eur. Phys. J. C* **72** (2012) 2151, doi:10.1140/epjc/s10052-012-2151-6, arXiv:1203.3172.
- [11] CMS Collaboration, “Search for pair production of first- and second-generation scalar leptoquarks in pp collisions at $\sqrt{s} = 7$ TeV”, *Phys. Rev. D* **86** (2012) 052013, doi:10.1103/PhysRevD.86.052013, arXiv:1207.5406.
- [12] D0 Collaboration, “Search for Third-Generation Scalar Leptoquarks in $p\bar{p}$ Collisions at $\sqrt{s} = 1.96$ TeV”, *Phys. Rev. Lett.* **99** (2007) 061801, doi:10.1103/PhysRevLett.99.061801, arXiv:0705.0812.
- [13] CDF Collaboration, “Search for third generation vector leptoquarks in $p\bar{p}$ collisions at $\sqrt{s} = 1.96$ TeV”, *Phys. Rev. D* **77** (2008) 091105, doi:10.1103/PhysRevD.77.091105, arXiv:0706.2832.
- [14] ATLAS Collaboration, “Search for third generation scalar leptoquarks in pp collisions at $\sqrt{s} = 7$ TeV with the ATLAS detector”, *JHEP* **06** (2013) 033, doi:10.1007/JHEP06(2013)033, arXiv:1303.0526.
- [15] CMS Collaboration, “Search for third-generation leptoquarks and scalar bottom quarks in pp collisions at $\sqrt{s} = 7$ TeV”, *JHEP* **12** (2012) 055, doi:10.1007/JHEP12(2012)055, arXiv:1210.5627.
- [16] CMS Collaboration, “Search for pair production of third-generation scalar leptoquarks and top squarks in proton-proton collisions at $\sqrt{s} = 8$ TeV”, *Phys. Lett. B* **739** (2014) 229, doi:10.1016/j.physletb.2014.10.063, arXiv:1408.0806.

- [17] CMS Collaboration, “Searches for third generation squark production in fully hadronic final states in proton-proton collisions at $\sqrt{s} = 8$ TeV”, (2015). arXiv:1503.08037. Submitted to *JHEP*.
- [18] R. Barbier et al., “*R*-Parity-violating supersymmetry”, *Phys. Rept.* **420** (2005) 1, doi:10.1016/j.physrep.2005.08.006, arXiv:hep-ph/0406039.
- [19] M. Krämer, T. Plehn, M. Spira, and P. M. Zerwas, “Pair production of scalar leptoquarks at the CERN LHC”, *Phys. Rev. D* **71** (2005) 057503, doi:10.1103/PhysRevD.71.057503, arXiv:hep-ph/0411038.
- [20] CMS Collaboration, “The CMS experiment at the CERN LHC”, *JINST* **3** (2008) S08004, doi:10.1088/1748-0221/3/08/S08004.
- [21] CMS Collaboration, “Particle-Flow Event Reconstruction in CMS and Performance for Jets, Taus, and E_T^{miss} ”, CMS Physics Analysis Summary CMS-PAS-PFT-09-001, 2009.
- [22] CMS Collaboration, “Commissioning of the Particle-flow Event Reconstruction with the first LHC collisions recorded in the CMS detector”, CMS Physics Analysis Summary CMS-PAS-PFT-10-001, 2010.
- [23] CMS Collaboration, “Performance of CMS muon reconstruction in pp collision events at $\sqrt{s} = 7$ TeV”, *JINST* **7** (2012) P10002, doi:10.1088/1748-0221/7/10/P10002, arXiv:1206.4071.
- [24] CMS Collaboration, “Performance of tau-lepton reconstruction and identification in CMS”, *JINST* **7** (2012) P01001, doi:10.1088/1748-0221/7/01/P01001, arXiv:1109.6034.
- [25] CMS Collaboration, “Performance of electron reconstruction and selection with the CMS detector in proton-proton collisions at $\sqrt{s} = 8$ TeV”, (2015). arXiv:1502.02701. Submitted to *JINST*.
- [26] M. Cacciari, G. P. Salam, and G. Soyez, “The anti- k_t jet clustering algorithm”, *JHEP* **04** (2008) 063, doi:10.1088/1126-6708/2008/04/063.
- [27] CMS Collaboration, “Determination of jet energy calibration and transverse momentum resolution in CMS”, *J. Instrum.* **6** (2011) P11002, doi:10.1088/1748-0221/6/11/P11002.
- [28] CMS Collaboration, “Performance of Missing Transverse Momentum Reconstruction Algorithms in Proton-Proton Collisions at $\sqrt{s} = 8$ TeV with the CMS Detector”, CMS Physics Analysis Summary CMS-PAS-JME-12-002, 2013.
- [29] CMS Collaboration, “The CMS high level trigger”, *Eur. Phys. J. C* **46** (2006) 605, doi:10.1140/epjc/s2006-02495-8, arXiv:hep-ex/0512077.
- [30] T. Sj “PYTHIA 6.4 physics and manual”, *JHEP* doi:10.1088/1126-6708/2006/05/026.
- [31] S. Alioli, P. Nason, C. Oleari, and E. Re, “A general framework for implementing NLO calculations in shower Monte Carlo programs: the POWHEG BOX”, *JHEP* **06** (2010) 043, doi:10.1007/JHEP06(2010)043, arXiv:1002.2581.

- [32] S. Alioli, P. Nason, C. Oleari, and E. Re, “NLO single-top production matched with shower in POWHEG: s - and t -channel contributions”, *JHEP* **09** (2009) 111, doi:10.1088/JHEP09(2009)111, arXiv:0907.4076. [Erratum: doi:10.1007/JHEP02(2010)011].
- [33] E. Re, “Single-top Wt -channel production matched with parton showers using the POWHEG method”, *Eur. Phys. J. C* **71** (2011) 1547, doi:10.1140/epjc/s10052-011-1547-z, arXiv:1009.2450.
- [34] S. Frixione, P. Nason, and G. Ridolfi, “A Positive-weight next-to-leading-order Monte Carlo for heavy flavour hadroproduction”, *JHEP* **09** (2007) 126, doi:10.1088/1126-6708/2007/09/126, arXiv:0707.3088.
- [35] J. Alwall et al., “MadGraph 5: going beyond”, *JHEP* **06** (2011) 128, doi:10.1007/JHEP06(2011)128, arXiv:1106.0522.
- [36] J. Alwall et al., “Comparative study of various algorithms for the merging of parton showers and matrix elements in hadronic collisions”, *Eur. Phys. J. C* **53** (2008) 473, doi:10.1140/epjc/s10052-007-0490-5, arXiv:0706.2569.
- [37] Z. Wąs, “TAUOLA the library for tau lepton decay, and KKMC/KORALB/KORALZ/... status report”, *Nucl. Phys. B, Proc. Suppl.* **98** (2001) 96, doi:10.1016/S0920-5632(01)01200-2.
- [38] GEANT4 Collaboration, “GEANT4—a simulation toolkit”, *Nucl. Instrum. Meth. A* **506** (2003) 250, doi:10.1016/S0168-9002(03)01368-8.
- [39] H.-L. Lai et al., “New parton distributions for collider physics”, *Phys. Rev. D* **82** (2010) 074024, doi:10.1103/PhysRevD.82.074024, arXiv:1007.2241.
- [40] J. Pumplin et al., “New generation of parton distributions with uncertainties from global QCD analysis”, *JHEP* **07** (2002) 012, doi:10.1088/1126-6708/2002/07/012, arXiv:hep-ph/0201195.
- [41] Y. Li and F. Petriello, “Combining QCD and electroweak corrections to dilepton production in FEWZ”, *Phys. Rev. D* **86** (2012) 094034, doi:10.1103/PhysRevD.86.094034, arXiv:1208.5967.
- [42] M. Czakon, P. Fiedler, and A. Mitov, “Total Top-Quark Pair-Production Cross Section at Hadron Colliders Through $O(\alpha_S^4)$ ”, *Phys. Rev. Lett.* **110** (2013) 252004, doi:10.1103/PhysRevLett.110.252004, arXiv:1303.6254.
- [43] O. Brein, R. V. Harlander, and T. J. E. Zirke, “vh@nnlo—Higgs Strahlung at hadron colliders”, *Comput. Phys. Commun.* **184** (2013) 998, doi:10.1016/j.cpc.2012.11.002, arXiv:1210.5347.
- [44] N. Kidonakis and R. Vogt, “Theoretical top quark cross section at the Tevatron and the LHC”, *Phys. Rev. D* **78** (2008) 074005, doi:10.1103/PhysRevD.78.074005, arXiv:0805.3844.
- [45] J. M. Campbell, R. K. Ellis, and C. Williams, “Vector boson pair production at the LHC”, *JHEP* **07** (2011) 018, doi:10.1007/JHEP07(2011)018, arXiv:1105.0020.

- [46] M. V. Garzelli, A. Kardos, C. G. Papadopoulos, and Z. Trócsányi, “ $t\bar{t}W^\pm$ and $t\bar{t}Z$ hadroproduction at NLO accuracy in QCD with Parton Shower and Hadronization effects”, *JHEP* **11** (2012) 056, doi:10.1007/JHEP11(2012)056, arXiv:1208.2665.
- [47] J. M. Campbell and R. K. Ellis, “ $t\bar{t}W^\pm$ production and decay at NLO”, *JHEP* **07** (2012) 052, doi:10.1007/JHEP07(2012)052, arXiv:1204.5678.
- [48] R. Frederix et al., “Scalar and pseudoscalar Higgs production in association with a top-antitop pair”, *Phys. Lett. B* **701** (2011) 427, doi:10.1016/j.physletb.2011.06.012, arXiv:1104.5613.
- [49] M. V. Garzelli, A. Kardos, C. G. Papadopoulos, and Z. Trócsányi, “Standard Model Higgs boson production in association with a top anti-top pair at NLO with parton showering”, *Europhys. Lett.* **96** (2011) 11001, doi:10.1209/0295-5075/96/11001, arXiv:1108.0387.
- [50] J. Alwall et al., “The automated computation of tree-level and next-to-leading order differential cross sections, and their matching to parton shower simulations”, *JHEP* **07** (2014) 079, doi:10.1007/JHEP07(2014)079, arXiv:1405.0301.
- [51] CMS Collaboration, “Measurement of differential top-quark pair production cross sections in pp collisions at $\sqrt{s} = 7$ TeV”, *Eur. Phys. J. C* **73** (2013) 2339, doi:10.1140/epjc/s10052-013-2339-4, arXiv:1211.2220.
- [52] CMS Collaboration, “Differential cross section measurements for the production of a W boson in association with jets in proton-proton collisions at $\sqrt{s} = 7$ TeV”, *Phys. Lett. B* **741** (2015) 12, doi:10.1016/j.physletb.2014.12.003, arXiv:1406.7533.
- [53] G. Punzi, “Sensitivity of searches for new signals and its optimization”, in *Statistical problems in particle physics, astrophysics, and cosmology (PHYSTAT2003)*, L. Lyons, R. P. Mount, and R. Reitmeyer, eds. 2003. arXiv:physics/0308063.
- [54] CMS Collaboration, “Measurement of the $t\bar{t}$ production cross section in the dilepton channel in pp collisions at $\sqrt{s} = 7$ TeV”, *JHEP* **11** (2012) 067, doi:10.1007/JHEP11(2012)067, arXiv:1208.2671.
- [55] CMS Collaboration, “Measurement of the $t\bar{t}$ production cross section in the dilepton channel in pp collisions at $\sqrt{s} = 8$ TeV”, *JHEP* **02** (2014) 024, doi:10.1007/JHEP02(2014)024, arXiv:1312.7582.
- [56] CMS Collaboration, “CMS Luminosity Based on Pixel Cluster Counting - Summer 2013 Update”, CMS Physics Analysis Summary CMS-PAS-LUM-13-001, 2013.
- [57] CMS Collaboration, “Measurement of the inclusive W and Z production cross sections in pp collisions at $\sqrt{s} = 7$ TeV”, *JHEP* **10** (2011) 132, doi:10.1007/JHEP10(2011)132, arXiv:1107.4789.
- [58] CMS Collaboration, “Measurement of the inelastic proton-proton cross section at $\sqrt{s} = 7$ TeV”, *Phys. Lett. B* **722** (2013) 5, doi:10.1016/j.physletb.2013.03.024, arXiv:1210.6718.
- [59] S. Alekhin et al., “The PDF4LHC Working Group Interim Report”, (2011). arXiv:1101.0536.

- [60] M. Botje et al., “The PDF4LHC Working Group Interim Recommendations”, (2011).
arXiv:1101.0538.
- [61] D. Bourilkov, R. C. Group, and M. R. Whalley, “LHAPDF: PDF use from the Tevatron to the LHC”, (2006). arXiv:hep-ph/0605240.
- [62] J. Ott. <http://www.theta-framework.org/>.

A The CMS Collaboration

Yerevan Physics Institute, Yerevan, Armenia

V. Khachatryan, A.M. Sirunyan, A. Tumasyan

Institut für Hochenergiephysik der OeAW, Wien, Austria

W. Adam, E. Asilar, T. Bergauer, J. Brandstetter, E. Brondolin, M. Dragicevic, J. Erö, M. Flechl, M. Friedl, R. Frühwirth¹, V.M. Ghete, C. Hartl, N. Hörmann, J. Hrubec, M. Jeitler¹, V. Knünz, A. König, M. Krammer¹, I. Krätschmer, D. Liko, I. Mikulec, D. Rabady², B. Rahbaran, H. Rohringer, J. Schieck¹, R. Schöfbeck, J. Strauss, W. Treberer-Treberspurg, W. Waltenberger, C.-E. Wulz¹

National Centre for Particle and High Energy Physics, Minsk, Belarus

V. Mossolov, N. Shumeiko, J. Suarez Gonzalez

Universiteit Antwerpen, Antwerpen, Belgium

S. Alderweireldt, T. Cornelis, E.A. De Wolf, X. Janssen, A. Knutsson, J. Lauwers, S. Luyckx, S. Ochesanu, R. Rougny, M. Van De Klundert, H. Van Haevermaet, P. Van Mechelen, N. Van Remortel, A. Van Spilbeek

Vrije Universiteit Brussel, Brussel, Belgium

S. Abu Zeid, F. Blekman, J. D'Hondt, N. Daci, I. De Bruyn, K. Deroover, N. Heracleous, J. Keaveney, S. Lowette, L. Moreels, A. Olbrechts, Q. Python, D. Strom, S. Tavernier, W. Van Doninck, P. Van Mulders, G.P. Van Onsem, I. Van Parijs

Université Libre de Bruxelles, Bruxelles, Belgium

P. Barria, C. Caillol, B. Clerboux, G. De Lentdecker, H. Delannoy, D. Dobur, G. Fasanella, L. Favart, A.P.R. Gay, A. Grebenyuk, A. Léonard, A. Mohammadi, L. Perniè, A. Randle-conde, T. Reis, T. Seva, L. Thomas, C. Vander Velde, P. Vanlaer, J. Wang, F. Zenoni

Ghent University, Ghent, Belgium

K. Beernaert, L. Benucci, A. Cimmino, S. Crucy, A. Fagot, G. Garcia, M. Gul, J. Mccartin, A.A. Ocampo Rios, D. Poyraz, D. Ryckbosch, S. Salva Diblen, M. Sigamani, N. Strobbe, F. Thyssen, M. Tytgat, W. Van Driessche, E. Yazgan, N. Zaganidis

Université Catholique de Louvain, Louvain-la-Neuve, Belgium

S. Basegmez, C. Beluffi³, O. Bondu, G. Bruno, R. Castello, A. Caudron, L. Ceard, G.G. Da Silva, C. Delaere, T. du Pree, D. Favart, L. Forthomme, A. Giammanco⁴, J. Hollar, A. Jafari, P. Jez, M. Komm, V. Lemaitre, A. Mertens, C. Nuttens, L. Perrini, A. Pin, K. Piotrkowski, A. Popov⁵, L. Quertenmont, M. Selvaggi, M. Vidal Marono

Université de Mons, Mons, Belgium

N. Beliy, G.H. Hammad

Centro Brasileiro de Pesquisas Fisicas, Rio de Janeiro, Brazil

W.L. Aldá Júnior, G.A. Alves, L. Brito, M. Correa Martins Junior, T. Dos Reis Martins, C. Hensel, C. Mora Herrera, A. Moraes, M.E. Pol, P. Rebello Teles

Universidade do Estado do Rio de Janeiro, Rio de Janeiro, Brazil

E. Belchior Batista Das Chagas, W. Carvalho, J. Chinellato⁶, A. Custódio, E.M. Da Costa, D. De Jesus Damiao, C. De Oliveira Martins, S. Fonseca De Souza, L.M. Huertas Guativa, H. Malbouisson, D. Matos Figueiredo, L. Mundim, H. Nogima, W.L. Prado Da Silva, J. Santaolalla, A. Santoro, A. Sznajder, E.J. Tonelli Manganote⁶, A. Vilela Pereira

Universidade Estadual Paulista ^a, Universidade Federal do ABC ^b, São Paulo, Brazil

S. Ahuja, C.A. Bernardes^b, S. Dogra^a, T.R. Fernandez Perez Tomei^a, E.M. Gregores^b, P.G. Mercadante^b, S.F. Novaes^a, Sandra S. Padula^a, D. Romero Abad, J.C. Ruiz Vargas

Institute for Nuclear Research and Nuclear Energy, Sofia, Bulgaria

A. Aleksandrov, V. Genchev², R. Hadjiiska, P. Iaydjiev, A. Marinov, S. Piperov, M. Rodozov, S. Stoykova, G. Sultanov, M. Vutova

University of Sofia, Sofia, Bulgaria

A. Dimitrov, I. Glushkov, L. Litov, B. Pavlov, P. Petkov

Institute of High Energy Physics, Beijing, China

M. Ahmad, J.G. Bian, G.M. Chen, H.S. Chen, M. Chen, T. Cheng, R. Du, C.H. Jiang, R. Plestina⁷, F. Romeo, S.M. Shaheen, J. Tao, C. Wang, Z. Wang

State Key Laboratory of Nuclear Physics and Technology, Peking University, Beijing, China

C. Asawatrangkuldee, Y. Ban, G. Chen, Q. Li, S. Liu, Y. Mao, S.J. Qian, D. Wang, M. Wang, Q. Wang, Z. Xu, D. Yang, F. Zhang⁸, L. Zhang, Z. Zhang, W. Zou

Universidad de Los Andes, Bogota, Colombia

C. Avila, A. Cabrera, L.F. Chaparro Sierra, C. Florez, J.P. Gomez, B. Gomez Moreno, J.C. Sanabria

University of Split, Faculty of Electrical Engineering, Mechanical Engineering and Naval Architecture, Split, Croatia

N. Godinovic, D. Lelas, D. Polic, I. Puljak

University of Split, Faculty of Science, Split, Croatia

Z. Antunovic, M. Kovac

Institute Rudjer Boskovic, Zagreb, Croatia

V. Brigljevic, K. Kadija, J. Luetic, L. Sudic

University of Cyprus, Nicosia, Cyprus

A. Attikis, G. Mavromanolakis, J. Mousa, C. Nicolaou, F. Ptochos, P.A. Razis, H. Rykaczewski

Charles University, Prague, Czech Republic

M. Bodlak, M. Finger, M. Finger Jr.⁹

Academy of Scientific Research and Technology of the Arab Republic of Egypt, Egyptian Network of High Energy Physics, Cairo, Egypt

A. Ali^{10,11}, R. Aly¹², S. Aly¹², S. Elgammal¹¹, A. Ellithi Kamel¹³, A. Lotfy¹⁴, M.A. Mahmoud¹⁴, R. Masod¹⁰, A. Radi^{11,10}

National Institute of Chemical Physics and Biophysics, Tallinn, Estonia

B. Calpas, M. Kadastik, M. Murumaa, M. Raidal, A. Tiko, C. Veelken

Department of Physics, University of Helsinki, Helsinki, Finland

P. Eerola, M. Voutilainen

Helsinki Institute of Physics, Helsinki, Finland

J. Härkönen, V. Karimäki, R. Kinnunen, T. Lampén, K. Lassila-Perini, S. Lehti, T. Lindén, P. Luukka, T. Mäenpää, T. Peltola, E. Tuominen, J. Tuominiemi, E. Tuovinen, L. Wendland

Lappeenranta University of Technology, Lappeenranta, Finland

J. Talvitie, T. Tuuva

DSM/IRFU, CEA/Saclay, Gif-sur-Yvette, France

M. Besancon, F. Couderc, M. Dejardin, D. Denegri, B. Fabbro, J.L. Faure, C. Favaro, F. Ferri, S. Ganjour, A. Givernaud, P. Gras, G. Hamel de Monchenault, P. Jarry, E. Locci, J. Malcles, J. Rander, A. Rosowsky, M. Titov, A. Zghiche

Laboratoire Leprince-Ringuet, Ecole Polytechnique, IN2P3-CNRS, Palaiseau, France

S. Baffioni, F. Beaudette, P. Busson, L. Cadamuro, E. Chapon, C. Charlot, T. Dahms, O. Davignon, N. Filipovic, A. Florent, R. Granier de Cassagnac, L. Mastrolorenzo, P. Miné, I.N. Naranjo, M. Nguyen, C. Ochando, G. Ortona, P. Paganini, S. Regnard, R. Salerno, J.B. Sauvan, Y. Sirois, T. Strebler, Y. Yilmaz, A. Zabi

Institut Pluridisciplinaire Hubert Curien, Université de Strasbourg, Université de Haute Alsace Mulhouse, CNRS/IN2P3, Strasbourg, France

J.-L. Agram¹⁵, J. Andrea, A. Aubin, D. Bloch, J.-M. Brom, M. Buttignol, E.C. Chabert, N. Chanon, C. Collard, E. Conte¹⁵, J.-C. Fontaine¹⁵, D. Gelé, U. Goerlach, C. Goetzmann, A.-C. Le Bihan, J.A. Merlin², K. Skovpen, P. Van Hove

Centre de Calcul de l'Institut National de Physique Nucleaire et de Physique des Particules, CNRS/IN2P3, Villeurbanne, France

S. Gadrat

Université de Lyon, Université Claude Bernard Lyon 1, CNRS-IN2P3, Institut de Physique Nucléaire de Lyon, Villeurbanne, France

S. Beauceron, N. Beaupere, C. Bernet⁷, G. Boudoul², E. Bouvier, S. Brochet, C.A. Carrillo Montoya, J. Chasserat, R. Chierici, D. Contardo, B. Courbon, P. Depasse, H. El Mamouni, J. Fan, J. Fay, S. Gascon, M. Gouzevitch, B. Ille, I.B. Laktineh, M. Lethuillier, L. Mirabito, A.L. Pequegnot, S. Perries, J.D. Ruiz Alvarez, D. Sabes, L. Sgandurra, V. Sordini, M. Vander Donckt, P. Verdier, S. Viret, H. Xiao

Institute of High Energy Physics and Informatization, Tbilisi State University, Tbilisi, Georgia

D. Lomidze

RWTH Aachen University, I. Physikalisches Institut, Aachen, Germany

C. Autermann, S. Beranek, M. Bontenackels, M. Edelhoff, L. Feld, A. Heister, M.K. Kiesel, K. Klein, M. Lipinski, A. Ostapchuk, M. Preuten, F. Raupach, J. Sammet, S. Schael, J.F. Schulte, T. Verlage, H. Weber, B. Wittmer, V. Zhukov⁵

RWTH Aachen University, III. Physikalisches Institut A, Aachen, Germany

M. Ata, M. Brodski, E. Dietz-Laursonn, D. Duchardt, M. Endres, M. Erdmann, S. Erdweg, T. Esch, R. Fischer, A. Güth, T. Hebbeker, C. Heidemann, K. Hoepfner, D. Klingebiel, S. Knutzen, P. Kreuzer, M. Merschmeyer, A. Meyer, P. Millet, M. Olschewski, K. Padeken, P. Papacz, T. Pook, M. Radziej, H. Reithler, M. Rieger, S.A. Schmitz, L. Sonnenschein, D. Teyssier, S. Thüer

RWTH Aachen University, III. Physikalisches Institut B, Aachen, Germany

V. Cherepanov, Y. Erdogan, G. Flügge, H. Geenen, M. Geisler, W. Haj Ahmad, F. Hoehle, B. Kargoll, T. Kress, Y. Kuessel, A. Künsken, J. Lingemann², A. Nowack, I.M. Nugent, C. Pistone, O. Pooth, A. Stahl

Deutsches Elektronen-Synchrotron, Hamburg, Germany

M. Aldaya Martin, I. Asin, N. Bartosik, O. Behnke, U. Behrens, A.J. Bell, K. Borras, A. Burgmeier, A. Cakir, L. Calligaris, A. Campbell, S. Choudhury, F. Costanza, C. Diez Pardos, G. Dolinska, S. Dooling, T. Dorland, G. Eckerlin, D. Eckstein, T. Eichhorn, G. Flucke, J. Garay

Garcia, A. Geiser, A. Gizhko, P. Gunnellini, J. Hauk, M. Hempel¹⁶, H. Jung, A. Kalogeropoulos, O. Karacheban¹⁶, M. Kasemann, P. Katsas, J. Kieseler, C. Kleinwort, I. Korol, W. Lange, J. Leonard, K. Lipka, A. Lobanov, R. Mankel, I. Marfin¹⁶, I.-A. Melzer-Pellmann, A.B. Meyer, G. Mittag, J. Mnich, A. Mussgiller, S. Naumann-Emme, A. Nayak, E. Ntomari, H. Perrey, D. Pitzl, R. Placakyte, A. Raspereza, P.M. Ribeiro Cipriano, B. Roland, M.Ö. Sahin, J. Salfeld-Nebgen, P. Saxena, T. Schoerner-Sadenius, M. Schröder, C. Seitz, S. Spannagel, C. Wissing

University of Hamburg, Hamburg, Germany

V. Blobel, M. Centis Vignali, A.R. Draeger, J. Erfle, E. Garutti, K. Goebel, D. Gonzalez, M. Görner, J. Haller, M. Hoffmann, R.S. Höing, A. Junkes, H. Kirschenmann, R. Klanner, R. Kogler, T. Lapsien, T. Lenz, I. Marchesini, D. Marconi, M. Meyer, D. Nowatschin, J. Ott, T. Peiffer, A. Perieanu, N. Pietsch, J. Poehlsen, D. Rathjens, C. Sander, H. Schettler, P. Schleper, E. Schlieckau, A. Schmidt, M. Seidel, V. Sola, H. Stadie, G. Steinbrück, H. Tholen, D. Troendle, E. Usai, L. Vanelderden, A. Vanhoefer

Institut für Experimentelle Kernphysik, Karlsruhe, Germany

M. Akbiyik, C. Barth, C. Baus, J. Berger, C. Böser, E. Butz, T. Chwalek, F. Colombo, W. De Boer, A. Descroix, A. Dierlamm, M. Feindt, F. Frensch, M. Giffels, A. Gilbert, F. Hartmann², U. Husemann, I. Katkov⁵, A. Kornmayer², P. Lobelle Pardo, M.U. Mozer, T. Müller, Th. Müller, M. Plagge, G. Quast, K. Rabbertz, S. Röcker, F. Roscher, H.J. Simonis, F.M. Stober, R. Ulrich, J. Wagner-Kuhr, S. Wayand, T. Weiler, C. Wöhrmann, R. Wolf

Institute of Nuclear and Particle Physics (INPP), NCSR Demokritos, Aghia Paraskevi, Greece

G. Anagnostou, G. Daskalakis, T. Gerasis, V.A. Giakoumopoulou, A. Kyriakis, D. Loukas, A. Markou, A. Psallidas, I. Topsis-Giotis

University of Athens, Athens, Greece

A. Agapitos, S. Kesisoglou, A. Panagiotou, N. Saoulidou, E. Tziaferi

University of Ioánnina, Ioánnina, Greece

I. Evangelou, G. Flouris, C. Foudas, P. Kokkas, N. Loukas, N. Manthos, I. Papadopoulos, E. Paradas, J. Strologas

Wigner Research Centre for Physics, Budapest, Hungary

G. Bencze, C. Hajdu, A. Hazi, P. Hidas, D. Horvath¹⁷, F. Sikler, V. Veszpremi, G. Vesztergombi¹⁸, A.J. Zsigmond

Institute of Nuclear Research ATOMKI, Debrecen, Hungary

N. Beni, S. Czellar, J. Karancsi¹⁹, J. Molnar, J. Palinkas, Z. Szillasi

University of Debrecen, Debrecen, Hungary

M. Bartók²⁰, A. Makovec, P. Raics, Z.L. Trocsanyi

National Institute of Science Education and Research, Bhubaneswar, India

P. Mal, K. Mandal, N. Sahoo, S.K. Swain

Panjab University, Chandigarh, India

S. Bansal, S.B. Beri, V. Bhatnagar, R. Chawla, R. Gupta, U. Bhawandeep, A.K. Kalsi, A. Kaur, M. Kaur, R. Kumar, A. Mehta, M. Mittal, N. Nishu, J.B. Singh

University of Delhi, Delhi, India

Ashok Kumar, Arun Kumar, A. Bhardwaj, B.C. Choudhary, A. Kumar, S. Malhotra, M. Naimuddin, K. Ranjan, R. Sharma, V. Sharma

Saha Institute of Nuclear Physics, Kolkata, India

S. Banerjee, S. Bhattacharya, K. Chatterjee, S. Dey, S. Dutta, B. Gomber, Sa. Jain, Sh. Jain, R. Khurana, N. Majumdar, A. Modak, K. Mondal, S. Mukherjee, S. Mukhopadhyay, A. Roy, D. Roy, S. Roy Chowdhury, S. Sarkar, M. Sharan

Bhabha Atomic Research Centre, Mumbai, India

A. Abdulsalam, D. Dutta, V. Jha, V. Kumar, A.K. Mohanty², L.M. Pant, P. Shukla, A. Topkar

Tata Institute of Fundamental Research, Mumbai, India

T. Aziz, S. Banerjee, S. Bhowmik²¹, R.M. Chatterjee, R.K. Dewanjee, S. Dugad, S. Ganguly, S. Ghosh, M. Guchait, A. Gurtu²², G. Kole, S. Kumar, M. Maity²¹, G. Majumder, K. Mazumdar, G.B. Mohanty, B. Parida, K. Sudhakar, N. Sur, B. Sutar, N. Wickramage²³

Indian Institute of Science Education and Research (IISER), Pune, India

S. Sharma

Institute for Research in Fundamental Sciences (IPM), Tehran, Iran

H. Bakhshiansohi, H. Behnamian, S.M. Etesami²⁴, A. Fahim²⁵, R. Goldouzian, M. Khakzad, M. Mohammadi Najafabadi, M. Naseri, S. Paktinat Mehdiabadi, F. Rezaei Hosseinabadi, B. Safarzadeh²⁶, M. Zeinali

University College Dublin, Dublin, Ireland

M. Felcini, M. Grunewald

INFN Sezione di Bari ^a, Università di Bari ^b, Politecnico di Bari ^c, Bari, Italy

M. Abbrescia^{a,b}, C. Calabria^{a,b}, C. Caputo^{a,b}, S.S. Chhibra^{a,b}, A. Colaleo^a, D. Creanza^{a,c}, L. Cristella^{a,b}, N. De Filippis^{a,c}, M. De Palma^{a,b}, L. Fiore^a, G. Iaselli^{a,c}, G. Maggi^{a,c}, M. Maggi^a, G. Miniello^{a,b}, S. My^{a,c}, S. Nuzzo^{a,b}, A. Pompili^{a,b}, G. Pugliese^{a,c}, R. Radogna^{a,b,2}, A. Ranieri^a, G. Selvaggi^{a,b}, A. Sharma^a, L. Silvestris^{a,2}, R. Venditti^{a,b}, P. Verwilligen^a

INFN Sezione di Bologna ^a, Università di Bologna ^b, Bologna, Italy

G. Abbiendi^a, C. Battilana, A.C. Benvenuti^a, D. Bonacorsi^{a,b}, S. Braibant-Giacomelli^{a,b}, L. Brigliadori^{a,b}, R. Campanini^{a,b}, P. Capiluppi^{a,b}, A. Castro^{a,b}, F.R. Cavallo^a, G. Codispoti^{a,b}, M. Cuffiani^{a,b}, G.M. Dallavalle^a, F. Fabbri^a, A. Fanfani^{a,b}, D. Fasanella^{a,b}, P. Giacomelli^a, C. Grandi^a, L. Guiducci^{a,b}, S. Marcellini^a, G. Masetti^a, A. Montanari^a, F.L. Navarria^{a,b}, A. Perrotta^a, A.M. Rossi^{a,b}, T. Rovelli^{a,b}, G.P. Siroli^{a,b}, N. Tosi^{a,b}, R. Travaglini^{a,b}

INFN Sezione di Catania ^a, Università di Catania ^b, CSFNSM ^c, Catania, Italy

G. Cappello^a, M. Chiorboli^{a,b}, S. Costa^{a,b}, F. Giordano^{a,c,2}, R. Potenza^{a,b}, A. Tricomi^{a,b}, C. Tuve^{a,b}

INFN Sezione di Firenze ^a, Università di Firenze ^b, Firenze, Italy

G. Barbagli^a, V. Ciulli^{a,b}, C. Civinini^a, R. D'Alessandro^{a,b}, E. Focardi^{a,b}, E. Gallo^a, S. Gonzi^{a,b}, V. Gori^{a,b}, P. Lenzi^{a,b}, M. Meschini^a, S. Paoletti^a, G. Sguazzoni^a, A. Tropiano^{a,b}, L. Viliani^{a,b}

INFN Laboratori Nazionali di Frascati, Frascati, Italy

L. Benussi, S. Bianco, F. Fabbri, D. Piccolo

INFN Sezione di Genova ^a, Università di Genova ^b, Genova, Italy

V. Calvelli^{a,b}, F. Ferro^a, M. Lo Vetere^{a,b}, E. Robutti^a, S. Tosi^{a,b}

INFN Sezione di Milano-Bicocca ^a, Università di Milano-Bicocca ^b, Milano, Italy

M.E. Dinardo^{a,b}, S. Fiorendi^{a,b}, S. Gennai^{a,2}, R. Gerosa^{a,b}, A. Ghezzi^{a,b}, P. Govoni^{a,b}, M.T. Lucchini^{a,b,2}, S. Malvezzi^a, R.A. Manzoni^{a,b}, B. Marzocchi^{a,b,2}, D. Menasce^a, L. Moroni^a, M. Paganoni^{a,b}, D. Pedrini^a, S. Ragazzi^{a,b}, N. Redaelli^a, T. Tabarelli de Fatis^{a,b}

INFN Sezione di Napoli ^a, Università di Napoli 'Federico II' ^b, Napoli, Italy, Università della Basilicata ^c, Potenza, Italy, Università G. Marconi ^d, Roma, Italy

S. Buontempo^a, N. Cavallo^{a,c}, S. Di Guida^{a,d,2}, M. Esposito^{a,b}, F. Fabozzi^{a,c}, A.O.M. Iorio^{a,b}, G. Lanza^a, L. Lista^a, S. Meola^{a,d,2}, M. Merola^a, P. Paolucci^{a,2}, C. Sciacca^{a,b}

INFN Sezione di Padova ^a, Università di Padova ^b, Padova, Italy, Università di Trento ^c, Trento, Italy

P. Azzi^{a,2}, N. Bacchetta^a, D. Bisello^{a,b}, A. Branca^{a,b}, R. Carlin^{a,b}, A. Carvalho Antunes De Oliveira^{a,b}, P. Checchia^a, M. Dall'Osso^{a,b}, T. Dorigo^a, F. Gasparini^{a,b}, U. Gasparini^{a,b}, A. Gozzelino^a, S. Lacaprara^a, M. Margoni^{a,b}, A.T. Meneguzzo^{a,b}, F. Montecassiano^a, M. Passaseo^a, J. Pazzini^{a,b}, N. Pozzobon^{a,b}, P. Ronchese^{a,b}, F. Simonetto^{a,b}, E. Torassa^a, M. Tosi^{a,b}, M. Zanetti^{a,b}, P. Zotto^{a,b}, A. Zucchetta^{a,b}, G. Zumerle^{a,b}

INFN Sezione di Pavia ^a, Università di Pavia ^b, Pavia, Italy

M. Gabusi^{a,b}, A. Magnani^a, S.P. Ratti^{a,b}, V. Re^a, C. Riccardi^{a,b}, P. Salvini^a, I. Vai^a, P. Vitulo^{a,b}

INFN Sezione di Perugia ^a, Università di Perugia ^b, Perugia, Italy

L. Alunni Solestizi^{a,b}, M. Biasini^{a,b}, G.M. Bilei^a, D. Ciangottini^{a,b,2}, L. Fanò^{a,b}, P. Lariccia^{a,b}, G. Mantovani^{a,b}, M. Menichelli^a, A. Saha^a, A. Santocchia^{a,b}, A. Spiezia^{a,b,2}

INFN Sezione di Pisa ^a, Università di Pisa ^b, Scuola Normale Superiore di Pisa ^c, Pisa, Italy

K. Androsov^{a,27}, P. Azzurri^a, G. Bagliesi^a, J. Bernardini^a, T. Boccali^a, G. Broccoli^{a,c}, R. Castaldi^a, M.A. Ciocci^{a,27}, R. Dell'Orso^a, S. Donato^{a,c,2}, G. Fedi, F. Fiori^{a,c}, L. Foà^{a,c†}, A. Giassi^a, M.T. Grippo^{a,27}, F. Ligabue^{a,c}, T. Lomtadze^a, L. Martini^{a,b}, A. Messineo^{a,b}, C.S. Moon^{a,28}, F. Palla^a, A. Rizzi^{a,b}, A. Savoy-Navarro^{a,29}, A.T. Serban^a, P. Spagnolo^a, P. Squillacioti^{a,27}, R. Tenchini^a, G. Tonelli^{a,b}, A. Venturi^a, P.G. Verdini^a

INFN Sezione di Roma ^a, Università di Roma ^b, Roma, Italy

L. Barone^{a,b}, F. Cavallari^a, G. D'imperio^{a,b}, D. Del Re^{a,b}, M. Diemoz^a, S. Gelli^{a,b}, C. Jorda^a, E. Longo^{a,b}, F. Margaroli^{a,b}, P. Meridiani^a, F. Micheli^{a,b}, G. Organtini^{a,b}, R. Paramatti^a, F. Preiato^{a,b}, S. Rahatlou^{a,b}, C. Rovelli^a, F. Santanastasio^{a,b}, L. Soffi^{a,b}, P. Traczyk^{a,b,2}

INFN Sezione di Torino ^a, Università di Torino ^b, Torino, Italy, Università del Piemonte Orientale ^c, Novara, Italy

N. Amapane^{a,b}, R. Arcidiacono^{a,c}, S. Argiro^{a,b}, M. Arneodo^{a,c}, R. Bellan^{a,b}, C. Biino^a, N. Cartiglia^a, S. Casasso^{a,b}, M. Costa^{a,b}, R. Covarelli^{a,b}, P. De Remigis^a, A. Degano^{a,b}, N. Demaria^a, L. Finco^{a,b,2}, B. Kiani^{a,b}, C. Mariotti^a, S. Maselli^a, E. Migliore^{a,b}, V. Monaco^{a,b}, M. Musich^a, M.M. Obertino^{a,c}, L. Pacher^{a,b}, N. Pastrone^a, M. Pelliccioni^a, G.L. Pinna Angioni^{a,b}, A. Romero^{a,b}, M. Ruspa^{a,c}, R. Sacchi^{a,b}, A. Solano^{a,b}, A. Staiano^a

INFN Sezione di Trieste ^a, Università di Trieste ^b, Trieste, Italy

S. Belforte^a, V. Candelise^{a,b,2}, M. Casarsa^a, F. Cossutti^a, G. Della Ricca^{a,b}, B. Gobbo^a, C. La Licata^{a,b}, M. Marone^{a,b}, A. Schizzi^{a,b}, T. Umer^{a,b}, A. Zanetti^a

Kangwon National University, Chunchon, Korea

S. Chang, A. Kropivnitskaya, S.K. Nam

Kyungpook National University, Daegu, Korea

D.H. Kim, G.N. Kim, M.S. Kim, D.J. Kong, S. Lee, Y.D. Oh, H. Park, A. Sakharov, D.C. Son

Chonbuk National University, Jeonju, Korea

H. Kim, T.J. Kim, M.S. Ryu

Chonnam National University, Institute for Universe and Elementary Particles, Kwangju, Korea

S. Song

Korea University, Seoul, Korea

S. Choi, Y. Go, D. Gyun, B. Hong, M. Jo, H. Kim, Y. Kim, B. Lee, K. Lee, K.S. Lee, S. Lee, S.K. Park, Y. Roh

Seoul National University, Seoul, Korea

H.D. Yoo

University of Seoul, Seoul, Korea

M. Choi, J.H. Kim, J.S.H. Lee, I.C. Park, G. Ryu

Sungkyunkwan University, Suwon, Korea

Y. Choi, Y.K. Choi, J. Goh, D. Kim, E. Kwon, J. Lee, I. Yu

Vilnius University, Vilnius, Lithuania

A. Juodagalvis, J. Vaitkus

National Centre for Particle Physics, Universiti Malaya, Kuala Lumpur, Malaysia

Z.A. Ibrahim, J.R. Komaragiri, M.A.B. Md Ali³⁰, F. Mohamad Idris, W.A.T. Wan Abdullah

Centro de Investigacion y de Estudios Avanzados del IPN, Mexico City, Mexico

E. Casimiro Linares, H. Castilla-Valdez, E. De La Cruz-Burelo, I. Heredia-de La Cruz, A. Hernandez-Almada, R. Lopez-Fernandez, G. Ramirez Sanchez, A. Sanchez-Hernandez

Universidad Iberoamericana, Mexico City, Mexico

S. Carrillo Moreno, F. Vazquez Valencia

Benemerita Universidad Autonoma de Puebla, Puebla, Mexico

S. Carpinteyro, I. Pedraza, H.A. Salazar Ibarguen

Universidad Autónoma de San Luis Potosí, San Luis Potosí, Mexico

A. Morelos Pineda

University of Auckland, Auckland, New Zealand

D. Krofcheck

University of Canterbury, Christchurch, New Zealand

P.H. Butler, S. Reucroft

National Centre for Physics, Quaid-I-Azam University, Islamabad, Pakistan

A. Ahmad, M. Ahmad, Q. Hassan, H.R. Hoorani, W.A. Khan, T. Khurshid, M. Shoaib

National Centre for Nuclear Research, Swierk, Poland

H. Bialkowska, M. Bluj, B. Boimska, T. Frueboes, M. Górski, M. Kazana, K. Nawrocki, K. Romanowska-Rybinska, M. Szleper, P. Zalewski

Institute of Experimental Physics, Faculty of Physics, University of Warsaw, Warsaw, Poland

G. Brona, K. Bunkowski, K. Doroba, A. Kalinowski, M. Konecki, J. Krolikowski, M. Misiura, M. Olszewski, M. Walczak

Laboratório de Instrumentação e Física Experimental de Partículas, Lisboa, Portugal

P. Bargassa, C. Beirão Da Cruz E Silva, A. Di Francesco, P. Faccioli, P.G. Ferreira Parracho, M. Gallinaro, L. Lloret Iglesias, F. Nguyen, J. Rodrigues Antunes, J. Seixas, O. Toldaiev, D. Vadrucio, J. Varela, P. Vischia

Joint Institute for Nuclear Research, Dubna, Russia

S. Afanasiev, P. Bunin, M. Gavrilenko, I. Golutvin, I. Gorbunov, A. Kamenev, V. Karjavin, V. Konoplyanikov, A. Lanev, A. Malakhov, V. Matveev³¹, P. Moisezenz, V. Palichik, V. Perelygin, S. Shmatov, S. Shulha, N. Skatchkov, V. Smirnov, T. Toriashvili³², A. Zarubin

Petersburg Nuclear Physics Institute, Gatchina (St. Petersburg), Russia

V. Golovtsov, Y. Ivanov, V. Kim³³, E. Kuznetsova, P. Levchenko, V. Murzin, V. Oreshkin, I. Smirnov, V. Sulimov, L. Uvarov, S. Vavilov, A. Vorobyev

Institute for Nuclear Research, Moscow, Russia

Yu. Andreev, A. Dermenev, S. Gninenko, N. Golubev, A. Karneyeu, M. Kirsanov, N. Krasnikov, A. Pashenkov, D. Tlisov, A. Toropin

Institute for Theoretical and Experimental Physics, Moscow, Russia

V. Epshteyn, V. Gavrillov, N. Lychkovskaya, V. Popov, I. Pozdnyakov, G. Safronov, A. Spiridonov, E. Vlasov, A. Zhokin

P.N. Lebedev Physical Institute, Moscow, Russia

V. Andreev, M. Azarkin³⁴, I. Dremin³⁴, M. Kirakosyan, A. Leonidov³⁴, G. Mesyats, S.V. Rusakov, A. Vinogradov

Skobeltsyn Institute of Nuclear Physics, Lomonosov Moscow State University, Moscow, Russia

A. Baskakov, A. Belyaev, E. Boos, M. Dubinin³⁵, L. Dudko, A. Ershov, A. Gribushin, V. Klyukhin, O. Kodolova, I. Lokhtin, I. Myagkov, S. Obraztsov, S. Petrushanko, V. Savrin, A. Snigirev

State Research Center of Russian Federation, Institute for High Energy Physics, Protvino, Russia

I. Azhgirey, I. Bayshev, S. Bitioukov, V. Kachanov, A. Kalinin, D. Konstantinov, V. Krychkin, V. Petrov, R. Ryutin, A. Sobol, L. Tourtchanovitch, S. Troshin, N. Tyurin, A. Uzunian, A. Volkov

University of Belgrade, Faculty of Physics and Vinca Institute of Nuclear Sciences, Belgrade, Serbia

P. Adzic³⁶, M. Ekmedzic, J. Milosevic, V. Rekovic

Centro de Investigaciones Energéticas Medioambientales y Tecnológicas (CIEMAT), Madrid, Spain

J. Alcaraz Maestre, E. Calvo, M. Cerrada, M. Chamizo Llatas, N. Colino, B. De La Cruz, A. Delgado Peris, D. Domínguez Vázquez, A. Escalante Del Valle, C. Fernandez Bedoya, J.P. Fernández Ramos, J. Flix, M.C. Fouz, P. Garcia-Abia, O. Gonzalez Lopez, S. Goy Lopez, J.M. Hernandez, M.I. Josa, E. Navarro De Martino, A. Pérez-Calero Yzquierdo, J. Puerta Pelayo, A. Quintario Olmeda, I. Redondo, L. Romero, M.S. Soares

Universidad Autónoma de Madrid, Madrid, Spain

C. Albajar, J.F. de Trocóniz, M. Missiroli, D. Moran

Universidad de Oviedo, Oviedo, Spain

H. Brun, J. Cuevas, J. Fernandez Menendez, S. Folgueras, I. Gonzalez Caballero, E. Palencia Cortezon, J.M. Vizan Garcia

Instituto de Física de Cantabria (IFCA), CSIC-Universidad de Cantabria, Santander, Spain

J.A. Brochero Cifuentes, I.J. Cabrillo, A. Calderon, J.R. Castiñeiras De Saa, J. Duarte Campderros, M. Fernandez, G. Gomez, A. Graziano, A. Lopez Virto, J. Marco, R. Marco,

C. Martinez Rivero, F. Matorras, F.J. Munoz Sanchez, J. Piedra Gomez, T. Rodrigo, A.Y. Rodríguez-Marrero, A. Ruiz-Jimeno, L. Scodellaro, I. Vila, R. Vilar Cortabitarte

CERN, European Organization for Nuclear Research, Geneva, Switzerland

D. Abbaneo, E. Auffray, G. Auzinger, M. Bachtis, P. Baillon, A.H. Ball, D. Barney, A. Benaglia, J. Bendavid, L. Benhabib, J.F. Benitez, G.M. Berruti, P. Bloch, A. Bocci, A. Bonato, C. Botta, H. Breuker, T. Camporesi, G. Cerminara, S. Colafranceschi³⁷, M. D'Alfonso, D. d'Enterria, A. Dabrowski, V. Daponte, A. David, M. De Gruttola, F. De Guio, A. De Roeck, S. De Visscher, E. Di Marco, M. Dobson, M. Dordevic, N. Dupont-Sagorin, A. Elliott-Peisert, G. Franzoni, W. Funk, D. Gigi, K. Gill, D. Giordano, M. Girone, F. Glege, R. Guida, S. Gundacker, M. Guthoff, J. Hammer, M. Hansen, P. Harris, J. Hegeman, V. Innocente, P. Janot, M.J. Kortelainen, K. Kousouris, K. Krajczar, P. Lecoq, C. Lourenço, N. Magini, L. Malgeri, M. Mannelli, J. Marrouche, A. Martelli, L. Masetti, F. Meijers, S. Mersi, E. Meschi, F. Moortgat, S. Morovic, M. Mulders, M.V. Nemallapudi, H. Neugebauer, S. Orfanelli, L. Orsini, L. Pape, E. Perez, A. Petrilli, G. Petrucciani, A. Pfeiffer, D. Piparo, A. Racz, G. Rolandi³⁸, M. Rovere, M. Ruan, H. Sakulin, C. Schäfer, C. Schwick, A. Sharma, P. Silva, M. Simon, P. Sphicas³⁹, D. Spiga, J. Steggemann, B. Stieger, M. Stoye, Y. Takahashi, D. Treille, A. Tsirou, G.I. Veres¹⁸, N. Wardle, H.K. Wöhri, A. Zagodzinska⁴⁰, W.D. Zeuner

Paul Scherrer Institut, Villigen, Switzerland

W. Bertl, K. Deiters, W. Erdmann, R. Horisberger, Q. Ingram, H.C. Kaestli, D. Kotlinski, U. Langenegger, T. Rohe

Institute for Particle Physics, ETH Zurich, Zurich, Switzerland

F. Bachmair, L. Bäni, L. Bianchini, M.A. Buchmann, B. Casal, G. Dissertori, M. Dittmar, M. Donegà, M. Dünser, P. Eller, C. Grab, C. Heidegger, D. Hits, J. Hoss, G. Kasieczka, W. Lustermann, B. Mangano, A.C. Marini, M. Marionneau, P. Martinez Ruiz del Arbol, M. Masciovecchio, D. Meister, N. Mohr, P. Musella, F. Nessi-Tedaldi, F. Pandolfi, J. Pata, F. Pauss, L. Perrozzi, M. Peruzzi, M. Quittnat, M. Rossini, A. Starodumov⁴¹, M. Takahashi, V.R. Tavolaro, K. Theofilatos, R. Wallny, H.A. Weber

Universität Zürich, Zurich, Switzerland

T.K. Aarrestad, C. AMSler⁴², M.F. Canelli, V. Chiochia, A. De Cosa, C. Galloni, A. Hinzmann, T. Hreus, B. Kilminster, C. Lange, J. Ngadiuba, D. Pinna, P. Robmann, F.J. Ronga, D. Salerno, S. Taroni, Y. Yang

National Central University, Chung-Li, Taiwan

M. Cardaci, K.H. Chen, T.H. Doan, C. Ferro, M. Konyushikhin, C.M. Kuo, W. Lin, Y.J. Lu, R. Volpe, S.S. Yu

National Taiwan University (NTU), Taipei, Taiwan

P. Chang, Y.H. Chang, Y.W. Chang, Y. Chao, K.F. Chen, P.H. Chen, C. Dietz, U. Grundler, W.-S. Hou, Y. Hsiung, Y.F. Liu, R.-S. Lu, M. Miñano Moya, E. Petrakou, J.f. Tsai, Y.M. Tzeng, R. Wilken

Chulalongkorn University, Faculty of Science, Department of Physics, Bangkok, Thailand

B. Asavapibhop, G. Singh, N. Srimanobhas, N. Suwonjandee

Cukurova University, Adana, Turkey

A. Adiguzel, S. Cerci⁴³, C. Dozen, S. Girgis, G. Gokbulut, Y. Guler, E. Gurpinar, I. Hos, E.E. Kangal⁴⁴, A. Kayis Topaksu, G. Onengut⁴⁵, K. Ozdemir⁴⁶, S. Ozturk⁴⁷, B. Tali⁴³, H. Topakli⁴⁷, M. Vergili, C. Zorbilmez

Middle East Technical University, Physics Department, Ankara, Turkey

I.V. Akin, B. Bilin, S. Bilmis, B. Isildak⁴⁸, G. Karapinar⁴⁹, U.E. Surat, M. Yalvac, M. Zeyrek

Bogazici University, Istanbul, Turkey

E.A. Albayrak⁵⁰, E. Gülmez, M. Kaya⁵¹, O. Kaya⁵², T. Yetkin⁵³

Istanbul Technical University, Istanbul, Turkey

K. Cankocak, Y.O. Günaydin⁵⁴, F.I. Vardarli

Institute for Scintillation Materials of National Academy of Science of Ukraine, Kharkov, Ukraine

B. Grynyov

National Scientific Center, Kharkov Institute of Physics and Technology, Kharkov, Ukraine

L. Levchuk, P. Sorokin

University of Bristol, Bristol, United Kingdom

R. Aggleton, F. Ball, L. Beck, J.J. Brooke, E. Clement, D. Cussans, H. Flacher, J. Goldstein, M. Grimes, G.P. Heath, H.F. Heath, J. Jacob, L. Kreczko, C. Lucas, Z. Meng, D.M. Newbold⁵⁵, S. Paramesvaran, A. Poll, T. Sakuma, S. Seif El Nasr-storey, S. Senkin, D. Smith, V.J. Smith

Rutherford Appleton Laboratory, Didcot, United Kingdom

K.W. Bell, A. Belyaev⁵⁶, C. Brew, R.M. Brown, D.J.A. Cockerill, J.A. Coughlan, K. Harder, S. Harper, E. Olaiya, D. Petyt, C.H. Shepherd-Themistocleous, A. Thea, I.R. Tomalin, T. Williams, W.J. Womersley, S.D. Worm

Imperial College, London, United Kingdom

M. Baber, R. Bainbridge, O. Buchmuller, A. Bundock, D. Burton, M. Citron, D. Colling, L. Corpe, N. Cripps, P. Dauncey, G. Davies, A. De Wit, M. Della Negra, P. Dunne, A. Elwood, W. Ferguson, J. Fulcher, D. Futyan, G. Hall, G. Iles, G. Karapostoli, M. Kenzie, R. Lane, R. Lucas⁵⁵, L. Lyons, A.-M. Magnan, S. Malik, J. Nash, A. Nikitenko⁴¹, J. Pela, M. Pesaresi, K. Petridis, D.M. Raymond, A. Richards, A. Rose, C. Seez, P. Sharp[†], A. Tapper, K. Uchida, M. Vazquez Acosta, T. Virdee, S.C. Zenz

Brunel University, Uxbridge, United Kingdom

J.E. Cole, P.R. Hobson, A. Khan, P. Kyberd, D. Leggat, D. Leslie, I.D. Reid, P. Symonds, L. Teodorescu, M. Turner

Baylor University, Waco, USA

J. Dittmann, K. Hatakeyama, A. Kasmi, H. Liu, N. Pastika, T. Scarborough

The University of Alabama, Tuscaloosa, USA

O. Charaf, S.I. Cooper, C. Henderson, P. Rumerio

Boston University, Boston, USA

A. Avetisyan, T. Bose, C. Fantasia, D. Gastler, P. Lawson, D. Rankin, C. Richardson, J. Rohlf, J. St. John, L. Sulak, D. Zou

Brown University, Providence, USA

J. Alimena, E. Berry, S. Bhattacharya, D. Cutts, Z. Demiragli, N. Dhir, A. Ferapontov, A. Garabedian, U. Heintz, E. Laird, G. Landsberg, Z. Mao, M. Narain, S. Sagir, T. Sinthuprasith

University of California, Davis, Davis, USA

R. Breedon, G. Breto, M. Calderon De La Barca Sanchez, S. Chauhan, M. Chertok, J. Conway, R. Conway, P.T. Cox, R. Erbacher, M. Gardner, W. Ko, R. Lander, M. Mulhearn, D. Pellett, J. Pilot, F. Ricci-Tam, S. Shalhout, J. Smith, M. Squires, D. Stolp, M. Tripathi, S. Wilbur, R. Yohay

University of California, Los Angeles, USA

R. Cousins, P. Everaerts, C. Farrell, J. Hauser, M. Ignatenko, G. Rakness, D. Saltzberg, E. Takasugi, V. Valuev, M. Weber

University of California, Riverside, Riverside, USA

K. Burt, R. Clare, J. Ellison, J.W. Gary, G. Hanson, J. Heilman, M. Ivova Rikova, P. Jandir, E. Kennedy, F. Lacroix, O.R. Long, A. Luthra, M. Malberti, M. Olmedo Negrete, A. Shrinivas, S. Sumowidagdo, H. Wei, S. Wimpenny

University of California, San Diego, La Jolla, USA

J.G. Branson, G.B. Cerati, S. Cittolin, R.T. D'Agnolo, A. Holzner, R. Kelley, D. Klein, D. Kovalskyi, J. Letts, I. Macneill, D. Olivito, S. Padhi, C. Palmer, M. Pieri, M. Sani, V. Sharma, S. Simon, M. Tadel, Y. Tu, A. Vartak, S. Wasserbaech⁵⁷, C. Welke, F. Würthwein, A. Yagil, G. Zevi Della Porta

University of California, Santa Barbara, Santa Barbara, USA

D. Barge, J. Bradmiller-Feld, C. Campagnari, A. Dishaw, V. Dutta, K. Flowers, M. Franco Sevilla, P. Geffert, C. George, F. Golf, L. Gouskos, J. Gran, J. Incandela, C. Justus, N. Mccoll, S.D. Mullin, J. Richman, D. Stuart, W. To, C. West, J. Yoo

California Institute of Technology, Pasadena, USA

D. Anderson, A. Apresyan, A. Bornheim, J. Bunn, Y. Chen, J. Duarte, A. Mott, H.B. Newman, C. Pena, M. Pierini, M. Spiropulu, J.R. Vlimant, S. Xie, R.Y. Zhu

Carnegie Mellon University, Pittsburgh, USA

V. Azzolini, A. Calamba, B. Carlson, T. Ferguson, Y. Iiyama, M. Paulini, J. Russ, M. Sun, H. Vogel, I. Vorobiev

University of Colorado at Boulder, Boulder, USA

J.P. Cumalat, W.T. Ford, A. Gaz, F. Jensen, A. Johnson, M. Krohn, T. Mulholland, U. Nauenberg, J.G. Smith, K. Stenson, S.R. Wagner

Cornell University, Ithaca, USA

J. Alexander, A. Chatterjee, J. Chaves, J. Chu, S. Dittmer, N. Eggert, N. Mirman, G. Nicolas Kaufman, J.R. Patterson, A. Ryd, L. Skinnari, W. Sun, S.M. Tan, W.D. Teo, J. Thom, J. Thompson, J. Tucker, Y. Weng, P. Wittich

Fermi National Accelerator Laboratory, Batavia, USA

S. Abdullin, M. Albrow, J. Anderson, G. Apollinari, L.A.T. Bauerdick, A. Beretvas, J. Berryhill, P.C. Bhat, G. Bolla, K. Burkett, J.N. Butler, H.W.K. Cheung, F. Chlebana, S. Cihangir, V.D. Elvira, I. Fisk, J. Freeman, E. Gottschalk, L. Gray, D. Green, S. Grünendahl, O. Gutsche, J. Hanlon, D. Hare, R.M. Harris, J. Hirschauer, B. Hooberman, Z. Hu, S. Jindariani, M. Johnson, U. Joshi, A.W. Jung, B. Klima, B. Kreis, S. Kwan[†], S. Lammel, J. Linacre, D. Lincoln, R. Lipton, T. Liu, R. Lopes De Sá, J. Lykken, K. Maeshima, J.M. Marraffino, V.I. Martinez Outschoorn, S. Maruyama, D. Mason, P. McBride, P. Merkel, K. Mishra, S. Mrenna, S. Nahn, C. Newman-Holmes, V. O'Dell, O. Prokofyev, E. Sexton-Kennedy, A. Soha, W.J. Spalding, L. Spiegel, L. Taylor, S. Tkaczyk, N.V. Tran, L. Uplegger, E.W. Vaandering, C. Vernieri, M. Verzocchi, R. Vidal, A. Whitbeck, F. Yang, H. Yin

University of Florida, Gainesville, USA

D. Acosta, P. Avery, P. Bortignon, D. Bourilkov, A. Carnes, M. Carver, D. Curry, S. Das, G.P. Di Giovanni, R.D. Field, M. Fisher, I.K. Furic, J. Hugon, J. Konigsberg, A. Korytov, T. Kypreos, J.F. Low, P. Ma, K. Matchev, H. Mei, P. Milenovic⁵⁸, G. Mitselmakher, L. Muniz, D. Rank, A. Rinkevicius, L. Shchutska, M. Snowball, D. Sperka, S.J. Wang, J. Yelton

Florida International University, Miami, USA

S. Hewamanage, S. Linn, P. Markowitz, G. Martinez, J.L. Rodriguez

Florida State University, Tallahassee, USA

A. Ackert, J.R. Adams, T. Adams, A. Askew, J. Bochenek, B. Diamond, J. Haas, S. Hagopian, V. Hagopian, K.F. Johnson, A. Khatiwada, H. Prosper, V. Veeraraghavan, M. Weinberg

Florida Institute of Technology, Melbourne, USA

V. Bhopatkar, M. Hohlmann, H. Kalakhety, D. Mareskas-palcek, T. Roy, F. Yumiceva

University of Illinois at Chicago (UIC), Chicago, USA

M.R. Adams, L. Apanasevich, D. Berry, R.R. Betts, I. Bucinskaite, R. Cavanaugh, O. Evdokimov, L. Gauthier, C.E. Gerber, D.J. Hofman, P. Kurt, C. O'Brien, I.D. Sandoval Gonzalez, C. Silkworth, P. Turner, N. Varelas, Z. Wu, M. Zakaria

The University of Iowa, Iowa City, USA

B. Bilki⁵⁹, W. Clarida, K. Dilsiz, R.P. Gandrajula, M. Haytmyradov, V. Khristenko, J.-P. Merlo, H. Mermerkaya⁶⁰, A. Mestvirishvili, A. Moeller, J. Nachtman, H. Ogul, Y. Onel, F. Ozok⁵⁰, A. Penzo, S. Sen, C. Snyder, P. Tan, E. Tiras, J. Wetzel, K. Yi

Johns Hopkins University, Baltimore, USA

I. Anderson, B.A. Barnett, B. Blumenfeld, D. Fehling, L. Feng, A.V. Gritsan, P. Maksimovic, C. Martin, K. Nash, M. Osherson, M. Swartz, M. Xiao, Y. Xin

The University of Kansas, Lawrence, USA

P. Baringer, A. Bean, G. Benelli, C. Bruner, J. Gray, R.P. Kenny III, D. Majumder, M. Malek, M. Murray, D. Noonan, S. Sanders, R. Stringer, Q. Wang, J.S. Wood

Kansas State University, Manhattan, USA

I. Chakaberia, A. Ivanov, K. Kaadze, S. Khalil, M. Makouski, Y. Maravin, L.K. Saini, N. Skhirtladze, I. Svintradze

Lawrence Livermore National Laboratory, Livermore, USA

D. Lange, F. Rebassoo, D. Wright

University of Maryland, College Park, USA

C. Anelli, A. Baden, O. Baron, A. Belloni, B. Calvert, S.C. Eno, J.A. Gomez, N.J. Hadley, S. Jabeen, R.G. Kellogg, T. Kolberg, Y. Lu, A.C. Mignerey, K. Pedro, Y.H. Shin, A. Skuja, M.B. Tonjes, S.C. Tonwar

Massachusetts Institute of Technology, Cambridge, USA

A. Apyan, R. Barbieri, A. Baty, K. Bierwagen, S. Brandt, W. Busza, I.A. Cali, L. Di Matteo, G. Gomez Ceballos, M. Goncharov, D. Gulhan, M. Klute, Y.S. Lai, Y.-J. Lee, A. Levin, P.D. Luckey, C. McGinn, X. Niu, C. Paus, D. Ralph, C. Roland, G. Roland, G.S.F. Stephans, K. Sumorok, M. Varma, D. Velicanu, J. Veverka, J. Wang, T.W. Wang, B. Wyslouch, M. Yang, V. Zhukova

University of Minnesota, Minneapolis, USA

B. Dahmes, A. Finkel, A. Gude, S.C. Kao, K. Klapoetke, Y. Kubota, J. Mans, S. Nourbakhsh, R. Rusack, N. Tambe, J. Turkewitz

University of Mississippi, Oxford, USA

J.G. Acosta, S. Oliveros

University of Nebraska-Lincoln, Lincoln, USA

E. Avdeeva, K. Bloom, S. Bose, D.R. Claes, A. Dominguez, C. Fangmeier, R. Gonzalez Suarez,

R. Kamalieddin, J. Keller, D. Knowlton, I. Kravchenko, J. Lazo-Flores, F. Meier, J. Monroy, F. Ratnikov, J.E. Siado, G.R. Snow

State University of New York at Buffalo, Buffalo, USA

M. Alyari, J. Dolen, J. George, A. Godshalk, I. Iashvili, J. Kaisen, A. Kharchilava, A. Kumar, S. Rappoccio

Northeastern University, Boston, USA

G. Alverson, E. Barberis, D. Baumgartel, M. Chasco, A. Hortiangtham, A. Massironi, D.M. Morse, D. Nash, T. Orimoto, R. Teixeira De Lima, D. Trocino, R.-J. Wang, D. Wood, J. Zhang

Northwestern University, Evanston, USA

K.A. Hahn, A. Kubik, N. Mucia, N. Odell, B. Pollack, A. Pozdnyakov, M. Schmitt, S. Stoynev, K. Sung, M. Trovato, M. Velasco, S. Won

University of Notre Dame, Notre Dame, USA

A. Brinkerhoff, N. Dev, M. Hildreth, C. Jessop, D.J. Karmgard, N. Kellams, K. Lannon, S. Lynch, N. Marinelli, F. Meng, C. Mueller, Y. Musienko³¹, T. Pearson, M. Planer, R. Ruchti, G. Smith, N. Valls, M. Wayne, M. Wolf, A. Woodard

The Ohio State University, Columbus, USA

L. Antonelli, J. Brinson, B. Bylsma, L.S. Durkin, S. Flowers, A. Hart, C. Hill, R. Hughes, K. Kotov, T.Y. Ling, B. Liu, W. Luo, D. Puigh, M. Rodenburg, B.L. Winer, H.W. Wulsin

Princeton University, Princeton, USA

O. Driga, P. Elmer, J. Hardenbrook, P. Hebda, S.A. Koay, P. Lujan, D. Marlow, T. Medvedeva, M. Mooney, J. Olsen, P. Piroué, X. Quan, H. Saka, D. Stickland, C. Tully, J.S. Werner, A. Zuranski

Purdue University, West Lafayette, USA

V.E. Barnes, D. Benedetti, D. Bortoletto, L. Gutay, M.K. Jha, M. Jones, K. Jung, M. Kress, N. Leonardo, D.H. Miller, N. Neumeister, F. Primavera, B.C. Radburn-Smith, X. Shi, I. Shipsey, D. Silvers, J. Sun, A. Svyatkovskiy, F. Wang, W. Xie, L. Xu, J. Zablocki

Purdue University Calumet, Hammond, USA

N. Parashar, J. Stupak

Rice University, Houston, USA

A. Adair, B. Akgun, Z. Chen, K.M. Ecklund, F.J.M. Geurts, W. Li, B. Michlin, M. Northup, B.P. Padley, R. Redjimi, J. Roberts, J. Rorie, Z. Tu, J. Zabel

University of Rochester, Rochester, USA

B. Betchart, A. Bodek, P. de Barbaro, R. Demina, Y. Eshaq, T. Ferbel, M. Galanti, A. Garcia-Bellido, P. Goldenzweig, J. Han, A. Harel, O. Hindrichs, A. Khukhunaishvili, G. Petrillo, M. Verzetti, D. Vishnevskiy

The Rockefeller University, New York, USA

L. Demortier

Rutgers, The State University of New Jersey, Piscataway, USA

S. Arora, A. Barker, J.P. Chou, C. Contreras-Campana, E. Contreras-Campana, D. Duggan, D. Ferencek, Y. Gershtein, R. Gray, E. Halkiadakis, D. Hidas, E. Hughes, S. Kaplan, R. Kunnawalkam Elayavalli, A. Lath, S. Panwalkar, M. Park, S. Salur, S. Schnetzer, D. Sheffield, S. Somalwar, R. Stone, S. Thomas, P. Thomassen, M. Walker

University of Tennessee, Knoxville, USA

M. Foerster, K. Rose, S. Spanier, A. York

Texas A&M University, College Station, USA

O. Bouhali⁶¹, A. Castaneda Hernandez, M. Dalchenko, M. De Mattia, A. Delgado, S. Dildick, R. Eusebi, W. Flanagan, J. Gilmore, T. Kamon⁶², V. Krutelyov, R. Montalvo, R. Mueller, I. Osipenkov, Y. Pakhotin, R. Patel, A. Perloff, J. Roe, A. Rose, A. Safonov, I. Suarez, A. Tatarinov, K.A. Ulmer

Texas Tech University, Lubbock, USA

N. Akchurin, C. Cowden, J. Damgov, C. Dragoiu, P.R. Duerdo, J. Faulkner, K. Kovitangoon, S. Kunori, K. Lamichhane, S.W. Lee, T. Libeiro, S. Undleeb, I. Volobouev

Vanderbilt University, Nashville, USA

E. Appelt, A.G. Delannoy, S. Greene, A. Gurrola, R. Janjam, W. Johns, C. Maguire, Y. Mao, A. Melo, P. Sheldon, B. Snook, S. Tuo, J. Velkovska, Q. Xu

University of Virginia, Charlottesville, USA

M.W. Arenton, S. Boutle, B. Cox, B. Francis, J. Goodell, R. Hirosky, A. Ledovskoy, H. Li, C. Lin, C. Neu, E. Wolfe, J. Wood, F. Xia

Wayne State University, Detroit, USA

C. Clarke, R. Harr, P.E. Karchin, C. Kottachchi Kankanamge Don, P. Lamichhane, J. Sturdy

University of Wisconsin, Madison, USA

D.A. Belknap, D. Carlsmith, M. Cepeda, A. Christian, S. Dasu, L. Dodd, S. Duric, E. Friis, R. Hall-Wilton, M. Herndon, A. Hervé, P. Klabbers, A. Lanaro, A. Levine, K. Long, R. Loveless, A. Mohapatra, I. Ojalvo, T. Perry, G.A. Pierro, G. Polese, I. Ross, T. Ruggles, T. Sarangi, A. Savin, N. Smith, W.H. Smith, D. Taylor, N. Woods

†: Deceased

1: Also at Vienna University of Technology, Vienna, Austria

2: Also at CERN, European Organization for Nuclear Research, Geneva, Switzerland

3: Also at Institut Pluridisciplinaire Hubert Curien, Université de Strasbourg, Université de Haute Alsace Mulhouse, CNRS/IN2P3, Strasbourg, France

4: Also at National Institute of Chemical Physics and Biophysics, Tallinn, Estonia

5: Also at Skobeltsyn Institute of Nuclear Physics, Lomonosov Moscow State University, Moscow, Russia

6: Also at Universidade Estadual de Campinas, Campinas, Brazil

7: Also at Laboratoire Leprince-Ringuet, Ecole Polytechnique, IN2P3-CNRS, Palaiseau, France

8: Also at Université Libre de Bruxelles, Bruxelles, Belgium

9: Also at Joint Institute for Nuclear Research, Dubna, Russia

10: Also at Ain Shams University, Cairo, Egypt

11: Now at British University in Egypt, Cairo, Egypt

12: Now at Helwan University, Cairo, Egypt

13: Also at Cairo University, Cairo, Egypt

14: Now at Fayoum University, El-Fayoum, Egypt

15: Also at Université de Haute Alsace, Mulhouse, France

16: Also at Brandenburg University of Technology, Cottbus, Germany

17: Also at Institute of Nuclear Research ATOMKI, Debrecen, Hungary

18: Also at Eötvös Loránd University, Budapest, Hungary

19: Also at University of Debrecen, Debrecen, Hungary

20: Also at Wigner Research Centre for Physics, Budapest, Hungary

-
- 21: Also at University of Visva-Bharati, Santiniketan, India
 - 22: Now at King Abdulaziz University, Jeddah, Saudi Arabia
 - 23: Also at University of Ruhuna, Matara, Sri Lanka
 - 24: Also at Isfahan University of Technology, Isfahan, Iran
 - 25: Also at University of Tehran, Department of Engineering Science, Tehran, Iran
 - 26: Also at Plasma Physics Research Center, Science and Research Branch, Islamic Azad University, Tehran, Iran
 - 27: Also at Università degli Studi di Siena, Siena, Italy
 - 28: Also at Centre National de la Recherche Scientifique (CNRS) - IN2P3, Paris, France
 - 29: Also at Purdue University, West Lafayette, USA
 - 30: Also at International Islamic University of Malaysia, Kuala Lumpur, Malaysia
 - 31: Also at Institute for Nuclear Research, Moscow, Russia
 - 32: Also at Institute of High Energy Physics and Informatization, Tbilisi State University, Tbilisi, Georgia
 - 33: Also at St. Petersburg State Polytechnical University, St. Petersburg, Russia
 - 34: Also at National Research Nuclear University 'Moscow Engineering Physics Institute' (MEPhI), Moscow, Russia
 - 35: Also at California Institute of Technology, Pasadena, USA
 - 36: Also at Faculty of Physics, University of Belgrade, Belgrade, Serbia
 - 37: Also at Facoltà Ingegneria, Università di Roma, Roma, Italy
 - 38: Also at Scuola Normale e Sezione dell'INFN, Pisa, Italy
 - 39: Also at University of Athens, Athens, Greece
 - 40: Also at Warsaw University of Technology, Institute of Electronic Systems, Warsaw, Poland
 - 41: Also at Institute for Theoretical and Experimental Physics, Moscow, Russia
 - 42: Also at Albert Einstein Center for Fundamental Physics, Bern, Switzerland
 - 43: Also at Adiyaman University, Adiyaman, Turkey
 - 44: Also at Mersin University, Mersin, Turkey
 - 45: Also at Cag University, Mersin, Turkey
 - 46: Also at Piri Reis University, Istanbul, Turkey
 - 47: Also at Gaziosmanpasa University, Tokat, Turkey
 - 48: Also at Ozyegin University, Istanbul, Turkey
 - 49: Also at Izmir Institute of Technology, Izmir, Turkey
 - 50: Also at Mimar Sinan University, Istanbul, Istanbul, Turkey
 - 51: Also at Marmara University, Istanbul, Turkey
 - 52: Also at Kafkas University, Kars, Turkey
 - 53: Also at Yildiz Technical University, Istanbul, Turkey
 - 54: Also at Kahramanmaras Sütcü Imam University, Kahramanmaras, Turkey
 - 55: Also at Rutherford Appleton Laboratory, Didcot, United Kingdom
 - 56: Also at School of Physics and Astronomy, University of Southampton, Southampton, United Kingdom
 - 57: Also at Utah Valley University, Orem, USA
 - 58: Also at University of Belgrade, Faculty of Physics and Vinca Institute of Nuclear Sciences, Belgrade, Serbia
 - 59: Also at Argonne National Laboratory, Argonne, USA
 - 60: Also at Erzincan University, Erzincan, Turkey
 - 61: Also at Texas A&M University at Qatar, Doha, Qatar
 - 62: Also at Kyungpook National University, Daegu, Korea